Arabian Journal of Chemistry (2018) **11**, 353–369

King Saud University

Arabian Journal of Chemistry

www.ksu.edu.sa
www.sciencedirect.com

ORIGINAL ARTICLE

Hepatotoxicity and antioxidant activity of some new N,N′-disubstituted benzimidazole-2-thiones, radical scavenging mechanism and structure-activity relationship

Neda O. Anastassova [a], Anelia Ts. Mavrova [a,*], Denitsa Y. Yancheva [b,*], Magdalena S. Kondeva-Burdina [c], Virginia I. Tzankova [c], Simeon S. Stoyanov [b], Boris L. Shivachev [d], Rositsa P. Nikolova [d]

[a] *University of Chemical Technology and Metallurgy, 8 Kliment Ohridski Blvd., 1756 Sofia, Bulgaria*
[b] *Institute of Organic Chemistry with Centre of Phytochemistry, Bulgarian Academy of Sciences, Acad. G. Bonchev Str., Build. 9, 1113 Sofia, Bulgaria*
[c] *Drug Metabolism and Drug Toxicity Laboratory, Pharmacology, Pharmacotherapy and Toxicology Department, Faculty of Pharmacy, Medical University-Sofia, Bulgaria*
[d] *Acad. Ivan Kostov Institute of Mineralogy and Crystallography, Bulgarian Academy of Sciences, Acad. G. Bonchev Str., Build. 107, 1113 Sofia, Bulgaria*

Received 8 September 2016; revised 5 December 2016; accepted 6 December 2016
Available online 19 December 2016

KEYWORDS

1,3-Disubstituted benzimidazole-2-thiones;
Michael addition;
Hepatotoxicity;
Oxidative stress;
Radical scavenging;
DFT calculations

Abstract A new method for the synthesis of 1,3-disubstituted benzimidazole derivatives was developed using *aza*-Michael addition. The target compounds were synthesized in good yields and purity and tested on isolated hepatocytes for their toxicity and antioxidant activity. The antioxidant properties of the substances with lowest toxicity were evaluated using oxidative stress induced by *tert*-butyl hydroperoxide (*tert*-BOOH). Some of them as methyl 3-[3-(3-methoxy-3-oxopropyl)-5-benzoyl-2-thioxo-2,3-dihydro-1H-benzimidazol-1-yl]propanoate **10** and 1,3-bis[3-(hydrazinooxy)-3-oxopropyl]-5-benzoyl-1,3-dihydro-2H-benzimidazole-2-thione **15** exhibited statistically significant cytoprotective and antioxidant effects which were similar to those of quercetin. In order to estimate the influence of the structure on the biological properties, structural characterization of the studied compounds was performed by X-ray diffraction analysis and DFT methods. On the basis of the

* Corresponding authors at: Department of Organic Synthesis, University of Chemical Technology and Metallurgy, 8 Kliment Ohridski Blvd., 1756 Sofia, Bulgaria.
E-mail address: anmav@abv.bg (A.Ts. Mavrova).
Peer review under responsibility of King Saud University.

Production and hosting by Elsevier

http://dx.doi.org/10.1016/j.arabjc.2016.12.003
1878-5352 © 2016 The Authors. Production and hosting by Elsevier B.V. on behalf of King Saud University.
This is an open access article under the CC BY-NC-ND license (http://creativecommons.org/licenses/by-nc-nd/4.0/).

calculated reaction enthalpies of hydrogen atom abstraction (HAT mechanism) and single-electron transfer (SET mechanism) the mechanisms of the antioxidant action of the tested compounds were studied. Subsequently it was established that the HAT mechanism governs the radical scavenging of **10** and **15** in the lipid phase, while the SET mechanism is preferred in water medium for **10** and competitive to HAT for **15**.

© 2016 The Authors. Production and hosting by Elsevier B.V. on behalf of King Saud University. This is an open access article under the CC BY-NC-ND license (http://creativecommons.org/licenses/by-nc-nd/4.0/).

1. Introduction

The benzimidazole nucleus has attracted the attention of many researchers in biomedicinal and organic chemistry as a recognized pharmacophore exhibiting wide and versatile spectrum of biological activities. Structural modifications have brought out antiviral (Tonelli et al., 2008, 2010), antibacterial (Singh et al., 2012; Alasmary et al., 2015), anthelmintic (Mavrova et al., 2015), antihypertensive (Vyas and Ghate, 2010), analgesic (Monika et al., 2014; Achar et al., 2010), antitumor (Refaat, 2010; Huang et al., 2006; Farmanzadeh and Najafi, 2015), proton pump inhibiting (Shin and Kim, 2013), α-glucosidase and β-glucuronidase inhibiting (Zawawi et al., 2015, 2016; Taha et al., 2016; Kamil et al., 2015), and anticoagulant and antioxidant pharmacological properties (Arora et al., 2014; Kuş et al., 2004, 2010; Menteşea et al., 2015; Gurer-Orhan et al., 2006; Mavrova et al., 2015) that have found application in clinical practice. Leading therapeutic agents such as Enviradine, Albendazole, Thiabendazole, Omeprazole, Lansoprazole, Astemizole, and Telmisartan are examples of the vast potential of the benzimidazole structure. However, benzimidazole based antioxidants with medical application have not been discovered yet. The structural resemblance to melatonin and its N-substituted derivatives, which are powerful antioxidants (Galano et al., 2011; Phiphatwatcharaded et al., 2014; Shirinzadeh et al., 2010) has motivated us to focus on the study of 1,3-disubstituted benzimidazole-2-thiones.

Different lifestyle factors and exposure to environmental toxins affect the existing homeostatic balance in living organisms, which leads to excessive production of reactive oxygen species (ROS) and decreased antioxidant capacity. Oxidative stress is related to serious medical conditions such as cardiovascular diseases (Stephens and Priorm, 2015), diabetes (Maritim et al., 2003), cancer (Valko et al., 2006), neurodegenerative disorders (Halliwell, 2006) and DNA damage (Cooke et al., 2003). The lipid peroxidation caused by the initiation and propagation of ROS results in irreversible degrading modifications of the cell membrane and has been associated with pathogenesis of various liver diseases (Poli et al., 1987). Our group has recently reported the antioxidant activity of 1,3-disubstituted-benzimidazol-2-imines, which was investigated using a TBA–MDA test, where the highest inhibiting activity was shown by the derivative with a benzoyl functional group (Mavrova et al., 2015). In an effort to explore further the potential of 1,3-disubstituted-benzimidazole derivatives as antioxidant agents, we thought it is worthwhile to modify the benzimidazole ring into a corresponding benzimidazole-2-thione structure. The beneficiary role of sulfur functional groups for antioxidant action is well documented. The amino acid cysteine possessing a thiol functional group in the molecule has considerable cytoprotective properties when administered in rats before X-ray irradiation (Patt et al., 1949). An unusual sulfur-containing amino acid derivative of natural origin – ergothioneine, containing an imidazole ring, also acts as a physiologic antioxidant cytoprotectant (Paul and Snyder, 2010). 2-Mercaptobenzothiazole derivatives have demonstrated antioxidant activity toward the ABTS radical and radioprotective effect at LD 99.9/30 days-IRR (Harti et al., 2014). Introducing varied aryl and alkyl substituents at 1-position of the imidazole ring has yielded potent antioxidants (Kuş et al., 2008; Ayhan-Kilcigil et al., 2014). The crystal structures and intermolecular interactions of novel antioxidant triazolyl-benzmidazole derivatives have been determined and their radical scavenging mechanisms have been evaluated (Karayel et al., 2015).

Many routes for the synthesis of benzimidazole derivatives have been developed and modified in order to obtain products of high yields and purity (Grimmet, 1997; Basu and Mandal, 2015). However, there are very few reports on the synthesis of 1,3-disubstituted benzimidazole-2-thiones (El Ashry et al., 2016; Bespalov et al., 2015; Smith, 2008). An early report from 1982 stated the synthesis of a mixture of methyl 3-[3-(3-methoxy-3-oxopropyl)-2-thioxo-2,3-dihydro-1 H-benzimidazol-1-yl]propanoate (compound **6**) and methyl 3-(2-thioxo-2,3-dihydro-1H-benzimidazol-1-yl)propanoate (monosubstituted derivative of **6**) that were screened for insecticides (Saxena et al., 1982). In the present contribution, we propose an optimized novel set of conditions for the synthesis of novel N,N′-disubstituted benzimidazole-2-thiones using Michael addition, which has not been performed so far. The Michael addition is a simple reaction where a nucleophile (Michael donor) is added to an activated electrophilic 1,2-unsaturated compound (Michael acceptor). Our method uses lesser molar ratios and has shown to be very effective, favoring high conversion of the reactants, yielding only the desired disubstituted compounds with relatively fast reaction rates while performing a facile reproducible synthesis.

Hence in the present work we report a series of novel 1,3-disubstituted benzimidazole-2-thione derivatives synthesized by means of a new method using *aza*-Michael addition. The hepatotoxicity and the antioxidant activity of the compounds displaying the lowest toxicity were evaluated using oxidative stress induced by *tert*-butylhydroperoxide (*tert*-BuOOH) on rat liver cells. In order to obtain better understanding of the structure and its influence on the biological properties we applied computational DFT methods and X-ray crystallography analysis. The mechanisms of the antioxidant action of the tested compounds in nonpolar (lipid) and polar (aqueous) medium were studied based on calculated reaction enthalpies of hydrogen atom abstraction (HAT mechanism) and single-electron transfer (SET mechanism).

2. Results and discussions

2.1. Chemistry

The synthesis of the 1,3-disubstituted compounds was carried out as shown in Scheme 1.

The starting precursors **1**–**5** were synthesized by refluxing 4-substituted-1,2-diaminobenzenes, carbon disulfide, ethanol and potassium hydroxide according to the method described by us earlier (Mavrova et al., 2015). Compounds **1**–**5** may exist in thione and thiol form as depicted in Scheme 1 depending on the medium. In solid state, **1**–**5** were isolated as thiols (Supplementary Material).

The novel synthetic method for obtaining 5-substituted dimethyl 3,3′-(2-thioxo-1H-benzimidazole-1,3(2H)-diyl)dipropionates **6**–**10** utilizes the Michael addition of the starting compounds **1**–**5** to methyl acrylate. The reaction was carried out in

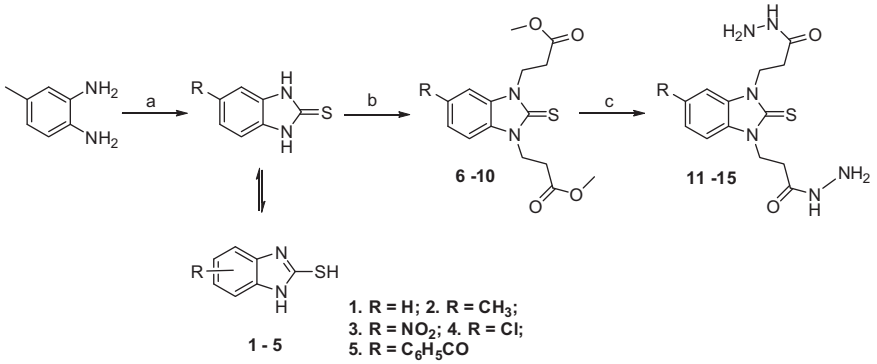

Scheme 1 Synthesis of the studied benzimidazole compounds. Reagents and conditions: (a) CS_2, KOH ethanol solution, refluxing; (b) methyl acrylate, DMF, refluxing; (c) hydrazine hydrate, ethanol solution, refluxing.

DMF media, where **1**–**5** are predominantly in thione form due to the solvent polarity. Our studies showed that for the preparation of 1,3-disubstituted benzimidazole-2-thiones the process could be carried out at a molar ratio of the starting reactants 1:2 (5-substituted benzimidazol-2-thiones:methyl acrylate). The reaction optimization conditions could be viewed on the following Table 1.

IR spectra, ^{1}H NMR and ^{13}C NMR confirmed that the benzimidazoles **1**–**5** reacted in their thione form and not as the thiol subsequently leading to the formation of 1,3-disubstituted derivatives **6**–**10**. In the ^{1}H NMR spectra, particularly meaningful are characteristic N—CH_2CH_2CO signals (triplets or double triplets) of the 1,3-substituted compounds shifted downfield due to the deshielding effect of both N-atoms and the CO groups. The chemical shift values for N—CH_2 for the esters varied in the range from 4.60 to 4.45 ppm while those for the CH_2—CO— groups were from 3.00 to 2.82 ppm depending on the solvent and the substituent in the benzimidazole ring.

The condensation in absolute ethanol medium of **6**–**10** with hydrazine hydrate in molar ratio 1:4 afforded hydrazides **11**–**15**. The chemical structures of the compounds and their purity were confirmed by IR-, ^{1}H NMR and ^{13}C NMR, DEPT, COSY and HSQC spectra and the results are presented in Section 4 and in the Supporting material. In the hydrazides group, analogously to the esters, the most typical are also the signals for the N—CH_2CH_2—CO-groups, as for the N—CH_2 groups the chemical shifts are in the range of 4.48 to 4.43 ppm and those for the CH_2—CO-group from 2.62 to 2.50 ppm. The labile NH protons are not characteristic and their chemical shifts depend on the water quantity in the solvent.

2.2. Pharmacology

2.2.1. Hepatotoxicity

Convenient well-controlled biological model systems with high drug-metabolizing capacities, which can be used in experimental toxicology, are isolated rat hepatocytes. This *in vitro* system

Table 1 Reaction optimization of Michael addition of compounds **1**–**5** to methyl acrylate.

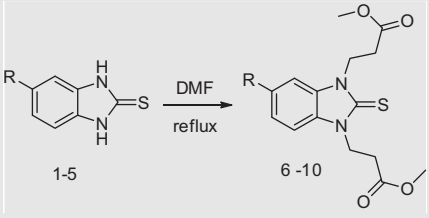

Entry	5-substituted benzimidazole-2-thione	Molar ratio to methyl acrylate	Temperature	Time (h)	Product (% yield) (%)
1.	**1**	1:11	100 °C	6	63
2.	**1**	1:11	Reflux	2	69
3.	**1**	1:6	Reflux	2	68
4.	**1**	1:2	Reflux	2	65
5.	**1**	1:2	100 °C	2	57
6.	**2**	1:11	Reflux	2	70
7.	**2**	1:2	Reflux	2	67
8.	**3**	1:11	Reflux	2	64
9.	**3**	1:2	Reflux	2	62
10.	**4**	1:11	Reflux	3	65
11.	**4**	1:2	Reflux	3	60
12.	**5**	1:11	Reflux	5	63
13.	**5**	1:2	Reflux	5	62

is part of the recommended tests from the European Centre for the Validation of Alternative Methods (ECVAM). The main goal of ECVAM was to promote the acceptance of alternative methods, which are important for reducing, refining and replacing the use of laboratory animals (Blaauboer et al., 1994). The studied benzimidazole-2-thiones were tested on isolated hepatocytes from male Wistar rats by a method providing a higher amount of live and metabolically active cells.

The effect of the compounds on the functional-metabolic status of the cells was assessed by monitoring the cell viability and changes in lactate dehydrogenase, glutathione and malondialdehyde levels. Lactate dehydrogenase (LDH) is a soluble cytoplasmic enzyme released into extracellular space when the plasma membrane is damaged. Therefore, in the present study the intracellular LDH leakage was used as an indicator of cell membrane integrity and cell viability of hepatocytes. It is well known that glutathione (GSH) is not only a reductant and one of the important antioxidants in the cells but also plays a mediator role in many physiologic processes, such as proliferation and apoptosis (Montserrat et al., 2009). Depletion of hepatic GSH was monitored as an indicator of mitochondria-associated apoptosis and oxidative stress. In light of the crucial role of oxidative stress in liver diseases, the oxidative stress in the isolated hepatocytes was monitored also by the production of malondialdehyde (MDA), which is the most abundant individual aldehyde resulting from the lipid peroxidation in biological systems. Increased MDA levels reveal elevated lipid peroxidation caused by overproduction of ROS. All the observed effects were compared to a control group of non-treated hepatocytes.

The studied compounds affected the functional-metabolic status of isolated rat hepatocytes to a different extent (Table 2).

As can be seen ester **10** (1,3-bis(methoxycarbonylethyl)-5-benzoyl-1,3-dihydro-2H-benzimidazol-2-thione) decreased cell viability only by 27**%** compared to non-treated hepatocytes, while **8** and **9** had much higher toxicity and induced statistically significant decrease in cell viability by 47% and 45%, respectively. The reduction in cell viability was related to membrane damage as evidenced by the detected LDH leakage. The cell membrane integrity was best preserved by incubation with compound **10** (a statistically significant increase in LDH leakage by 92%), which had no effect on the GSH levels and elevated the MDA production to the least extent (124%) among the esters. Incubation with chloro-derivative **9** induced the greatest LDH leakage among the ester derivatives – 334%, and the highest oxidative stress according to the MDA production (349% increase) and GSH depletion (53% decrease).

Among the hydrazides, compound **15** had the lowest hepatotoxic effects, while hydrazide **14** revealed the highest cytotoxicity (Table 1). Derivative **15** induced a statistically significant decrease in cell viability by only 21% and showed no toxic effect on the GSH level. When considering the effects of compound **15** it should be pointed out that it exhibited the lowest levels of LDH leakage and MDA production – 75% and 112% respectively, not only among the hydrazides, but within the group of all tested benzimidazole-2-thiones.

The reduced cell viability (47%) resulting from incubation with the chloro-substituted hydrazide **14** was accompanied by the highest detected LDH leakage (348%), GSH depletion (58%) and MDA production (388%). Obviously, this compound induced the highest oxidative stress in the isolated rat hepatocytes resulting in membrane damage and cell death.

The differences in the toxicity are due to the presence of different substituents in 5-th position of the benzimidazole ring. In the ester group the toxicity increased in direction **10** (benzoyl group) < **7** (methyl group) < **6** (unsubstituted) < **8** (nitro group) < **9** (chloro group). The same relationship was observed in the hydrazides group.

The ester **10** and the hydrazide **15**, which revealed the lowest cytotoxic effects on isolated rat hepatocytes, were examined for possible antioxidant activity in *tert*-butyl hydroperoxide-induced oxidative stress. Effects were compared to those of Quercetin – a well-known antioxidant (Fig. 1).

Administered alone, in concentration 75 μM, *tert*-butyl hydroperoxide showed statistically significant cytotoxic effects on isolated rat hepatocytes – decreased cell viability and GSH level by 78% and 79% respectively, and increased LDH leakage and MDA production by 458% and 476% respectively, compared to non-treated hepatocytes. The antioxidant activity of compounds **10** and **15** was estimated based on the comparison of the above-mentioned parameters with the hepatocytes treated with the *tert*-butyl hydroperoxide toxic agent in combination with **10** and **15**. The ester derivative **10** preserved cell

Table 2 Effects of the tested compounds in concentration of 250 μM on the parameters characterizing the functional-metabolic status of isolated rat hepatocytes.

Group	Cell viability (%)	LDH (μmol/min/10^6 cell)	GSH (nmol/10^6 cell)	MDA (nmol/10^6 cell)
Control	85 ± 1.0	0.117 ± 0.004	19 ± 1.5	0.049 ± 0.01
6	49 ± 3.6**	0.366 ± 0.03**	11 ± 1.2**	0.125 ± 0.003*
7	53 ± 3.1**	0.338 ± 0.02**	12 ± 1.5**	0.121 ± 0.01*
8	47 ± 2.6**	0.452 ± 0.01**	11 ± 3.1**	0.128 ± 0.003*
9	45 ± 1.0**	0.507 ± 0.01***	9 ± 1.5***	0.220 ± 0.02***
10	63 ± 3.1*	0.225 ± 0.01*	16 ± 2.1	0.110 ± 0.01*
11	50 ± 6.0**	0.260 ± 0.04*	12 ± 1.8**	0.111 ± 0.01*
12	66 ± 4.5*	0.222 ± 0.01*	12 ± 1.5*	0.107 ± 0.01*
13	48 ± 4.5**	0.434 ± 0.01**	11 ± 1.2**	0.148 ± 0.03**
14	45 ± 1.5**	0.524 ± 0.01***	8 ± 2.1***	0.239 ± 0.01***
15	67 ± 2.6*	0.205 ± 0.01*	16 ± 2.5	0.104 ± 0.01*

* $P < 0.05$.
** $P < 0.01$.
*** $P < 0.001$ vs control (non-treated hepatocytes).

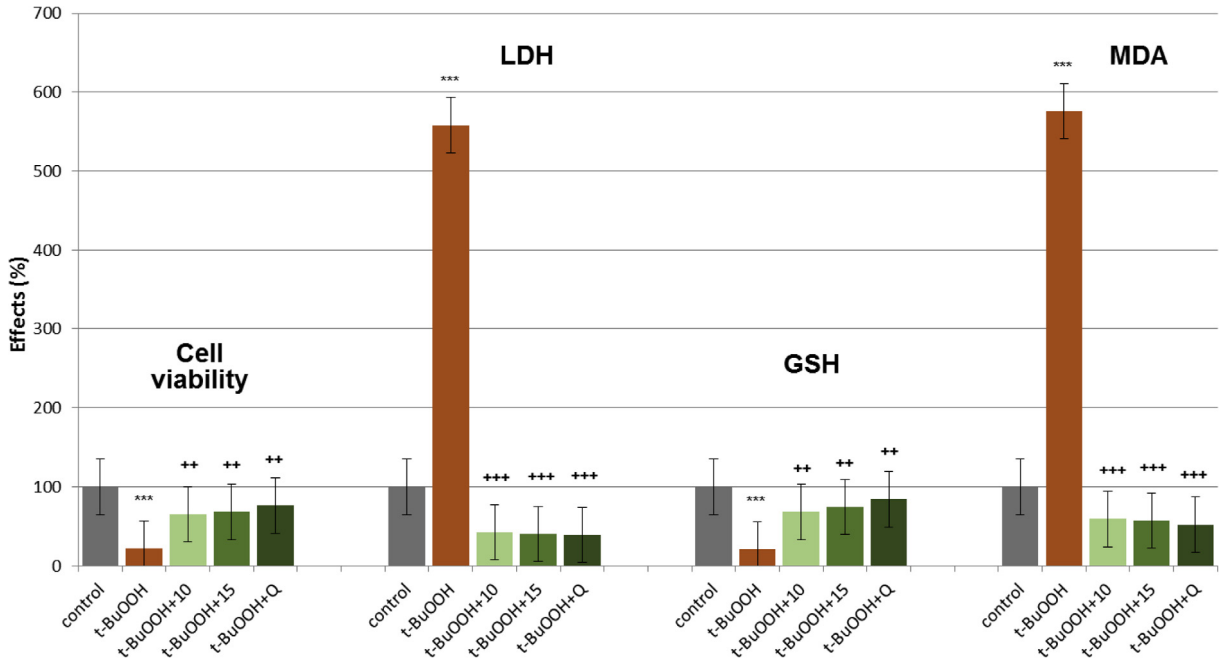

Figure 1 Effects of **10**, **15** and Quercetin (250 μM) on *tert*-butyl hydroperoxide (75 μM)-induced oxidative stress on parameters, characterizing the functional-metabolic status of isolated rat hepatocytes. $^{***}P < 0.001$ – vs control; $^{++}P < 0.01$, $^{+++}P < 0.001$ – vs *tert*-butyl hydroperoxide $^{***}P < 0.001$ – vs control group (non-treated hepatocytes); $^{++}P < 0.01$, $^{+++}P < 0.001$ – vs *tert*-butyl hydroperoxide.

viability and GSH level with 189% and 225% respectively, while **15** preserved these parameters with 205% and 250%. Concerning LDH leakage and MDA level, **10** decreased them by 58% and 41% respectively, while **15** – by 60% and 43%. Quercetin in this model preserved cell viability and GSH level with 242% and 300% respectively, and decreased LDH leakage and MDA production by 61% and 48% respectively.

In *tert*-butyl hydroperoxide (*t*-BuOOH) induced oxidative stress, ester **10** and hydrazide **15** revealed statistically significant cytoprotective and antioxidant effects similar to those of quercetin (Fig. 1).

The metabolism of *tert*-BuOOH to free radicals passes through several steps. In microsomal suspension (in the absence of NADPH), *tert*-BuOOH undergoes one-electron oxidation to a peroxyl radical (reaction (1)), whereas in the presence of NADPH – one-electron reduction to an alkoxyl radical (reaction (2)). The toxic agent undergoes β-scission to methyl radical (reaction (3)) in isolated mitochondria and intact cells. All these radicals cause lipid peroxidation (Ollinger and Brunk, 1995; O'Donell and Burkit, 1994).

$$(CH_3)_3CCOOH \rightarrow (CH_3)_3CCOO^{\cdot} + e^- + H^+ \qquad \text{(reaction1)}$$

$$(CH_3)_3CCOOH + e^- \rightarrow (CH_3)_3CCO^{\cdot} + OH^- \qquad \text{(reaction2)}$$

$$(CH_3)_3CCO^{\cdot} \rightarrow (CH_3)_2CCO + {}^{\cdot}CH_3 \qquad \text{(reaction3)}$$

The cytoprotective effects of compounds **10** and **15** on *t*-BuOOH-induced oxidative stress can be attributed to their activity as scavengers of ROS and influence on the metabolism of *tert*-butyl hydroperoxide. As a result, both compounds were able to reduce the lipid peroxidation, upregulate the GSH levels and protect the cell membrane integrity in the rat hepatocytes.

2.3. Single-Crystal X-ray diffraction analysis

For better understanding of the structure and its influence on the biological properties, structural characterization of the studied compounds was performed by X-ray diffraction analysis and DFT methods. Two of the ester derivatives, **6** and **10**, gave crystals suitable for X-ray diffraction analysis and enabled crystal structure determination. Compound **6** crystallized in the triclinic space group *P-1*, (No. 2) while compound **10** crystallized in the monoclinic space group $P2_1/n$ (No. 14), both with one molecule per asymmetric unit (Figs. 2a and 2b, Table 5 in Section 4).

The majority of the bond lengths and angles of **6** and **10** are comparable to those of similar structures (Jishkariani et al., 2013; Mohamed et al., 2009; Hahn et al., 2005; Mairesse et al., 1984; Ito et al., 1987; Kutzke et al., 1996) found in the CSD (Table 3).

The benzimidazole-2-thione and benzoyl rings are nearly planar with rmsd of 0.007, 0.006 and 0.004 Å in **6** and **10** respectively. The steric repulsion of the ortho H atoms of the benzimidazole-2-thione and benzoyl moieties in **10** leads to a twist of the rings as typically observed in benzoyl substituted aromatic compounds (Cox et al., 2008). The angle of 50.88 (7)° between the mean planes of the two rings corresponds to that in 4,4′-bis(diethylamino)benzophenone, 3,4-dihydroxybenzophenone and 3-hydroxybenzophenone. The benzoyl oxygen (016) is either below or above the mean planes of the two ring systems −0.676(4) and 0.539(3) Å.

Interestingly, the N-alkyl chains are in *trans* position (facing the opposite sides of the plane formed by the benzimidazole fragment) in **6**, while they are *cis* (facing the same side of the plane) in **10**. While no typical hydrogen bonding

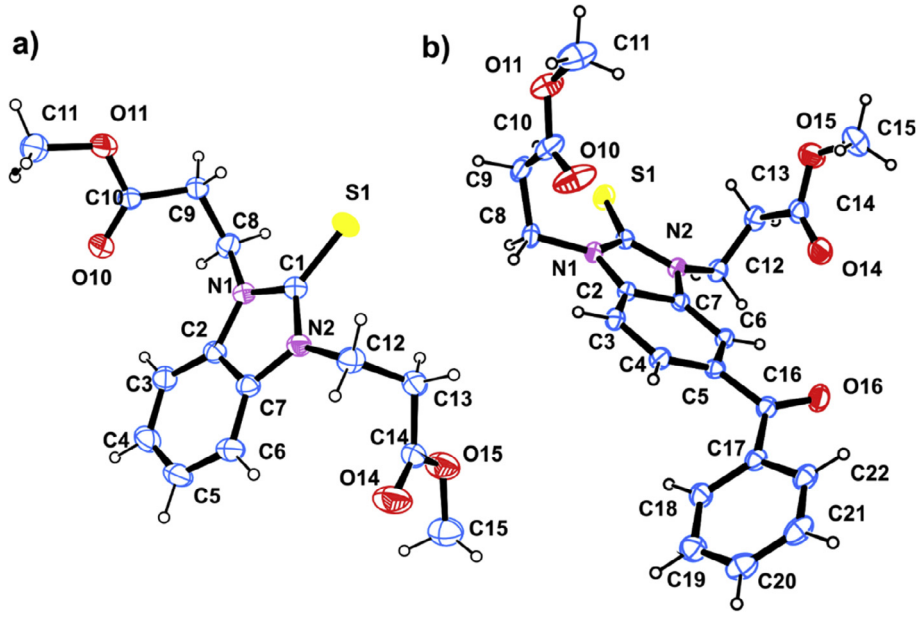

Figure 2a *ORTEP* drawing of (a) **6** and (b) **10** (atomic displacement ellipsoids are at 50% probability), the hydrogen atoms are shown as small spheres of arbitrary radii.

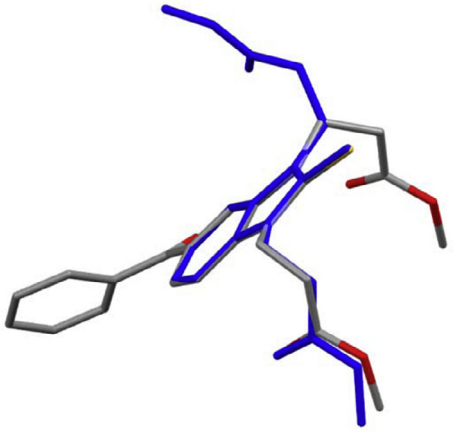

Figure 2b Overlay of the molecules of **6** (in blue/dark) and **10**.

interactions could be detected in the crystal structures of **6** and **10**, a multitude of weak interactions can be identified (Table 2). Among those, two intramolecular C—H···S and C—H···O (or π···O) interactions (Fig. 3) certainly play an essential role for the stabilization of the molecular geometry and the resulting conformation.

From the intermolecular weak interactions contributing to the crystal structure stabilization of **6** one should note the C13H13B···O10 producing chain propagation along *c*. The chains are linked by C5H5···O11 to form pseudo-layers parallel to *bc* (Fig. S1a). The pseudo-layers are stacked and connected by CH···S and CH···O and thus the crystal structure is stabilized by a complex network of weak interactions (Fig. S1b). Similar to **6**, in **10** the crystal structure stabilization is also achieved through a complex network of weak interactions (Fig. S2). However, due to the benzoyl fragment some additional CH3···π and CH···O interactions are observed.

2.4. Molecular geometry

As evidenced by the X-ray analysis, the 1,3-disubstituted benzimidazole-2-thiones have flexible N-alkyl chains able to occupy different positions. In order to find the preferred geometry of 1,3-disubstituted benzimidazole-2-thiones in isolated state, a large number of probable conformations were constructed and optimized at B3LYP/6-311++G** level of theory. For every structure, the stationary points found on the molecular potential energy hypersurfaces were characterized using standard analytical harmonic vibrational analysis. The absence of imaginary frequencies, as well as of negative

Table 3 Selected bond distances and angles for **6** and **10** (numbering is according to Fig. 2).

Bond length (Å)			Torsion angle (°)		
	6	**10**		**6**	**10**
C1═S1	1.671(2)	1.668(2)	C1—N1—C8—C9	75.4(2)	75.6(2)
C10—O10	1.183(3)	1.193(3)	N1—C8—C9—C10	73.5(2)	61.9(3)
C10—O11	1.321(3)	1.330(3)	C1—N2—C12—C13	82.7(2)	−82.3(2)
C14—O14	1.198(3)	1.197(3)	N2—C12—C13—C14	82.9(2)	−67.0(3)
C14—O15	1.309(3)	1.322(3)			

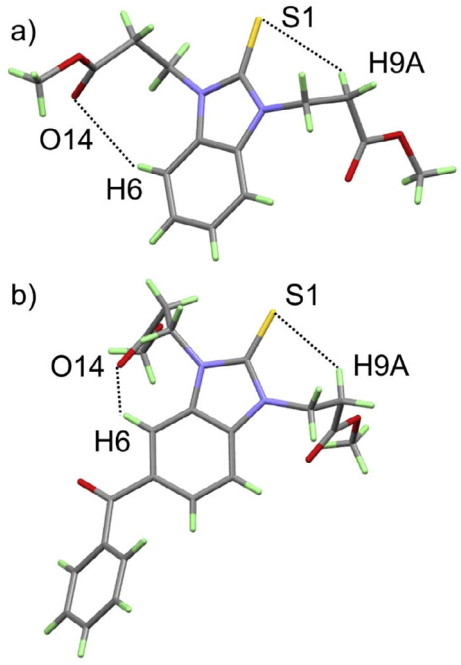

Figure 3 Observed weak interactions in **6** and **10** stabilizing the molecular geometry, S1···H9A: 2.784 Å (**6**) and 2.876 Å (**10**); O14···H6: 2.738 Å (**6**) and 2.601 Å (**10**).

eigenvalues of the second-derivative matrix, confirmed that the stationary points correspond to minima on the potential energy hypersurface. The benzimidazole-2-thione fragment is characterized by a planar structure, while the alkyl chains attached to N1 and N3 produce several extended and folded conformations and mutual orientations. It was found that bent conformation of the alkyl chain with the carbonyl ester group pointing to the benzimidazole moiety is the most favorable disposition of the N-substituents in isolated state. For the simplest ester and hydrazide derivatives (**6** and **11**) with an unsubstituted benzimidazole fragment, two stereoisomers are possible according to the mutual orientations of the N-alkyl chains (Scheme 2).

The stereoisomer with N-substituents in *trans* conformation is more favorable than that with N-alkyl chains in *cis* conformation. The conformational interconversion is related to a strong change in polarity, from 1.62 D for the *trans* form to 3.21 D for the *cis* form of compound **6**. The predicted isolated-state *trans* conformation of **6** is very similar to the one found in crystal state (Fig. S3a), with rmsd value of 0.2427 Å.

In all other studied derivatives the presence of a substituent at 5-position of the benzimidazole fragment creates two distinct faces of the plane of symmetry, which results in four possible stereoisomers (Scheme S1). In the case of benzoyl substituted derivatives (ester **10** and hydrazide **15**), the number of possible stereoisomers is increased by rotation of the benzoyl group. For each of the above mentioned stereoisomers there are four possible conformations of the benzoyl group (Scheme S2). The energy differences (0.05–0.40 kJ·mol^{-1}) between the stereoisomers resulting from the different orientation of the N-alkyl chains indicated that the side chains of the studied benzimidazole-2-thione derivatives are extremely flexible and the conversion of one form into another has very low energy requirements. Rotation of the benzoyl group also gave rise to stereoisomers with small energy differences (0.05–2.36 kJ·mol^{-1}). Comparing the total energies of the possible conformers of **10** and **15**, it was established that *trans* conformation is the preferred one for both molecules in isolated state (Scheme 3).

The angles between the mean planes of the benzimidazole-2-thione and benzoyl moieties in the optimized structures are 50° (**10**) and 54.8° (**15**), respectively.

The calculation results point out that the isolated-state structure of **10** differs from the crystal-state one (Fig. S3b). As is well-known, the crystal packing is affected by the formation of classical and non-classical hydrogen bonding, ring–ring (π···π) interactions, X—H···π interactions and other non-bonded intermolecular contacts influence. Thus considering

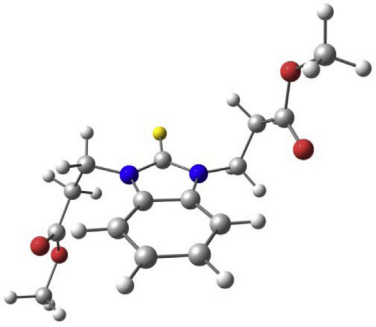

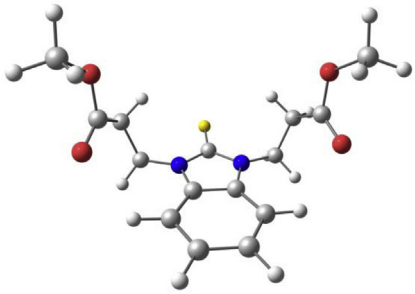

	6 (*trans* conformation)	**6** (*cis* conformation)
E_{tot}	-1391.384446 a.u.	-1391.384349 a.u.
ΔE	0.00	0.25 kJ.mol^{-1}
μ	1.62 D	3.21 D

Scheme 2 Possible stereoisomers of **6**.

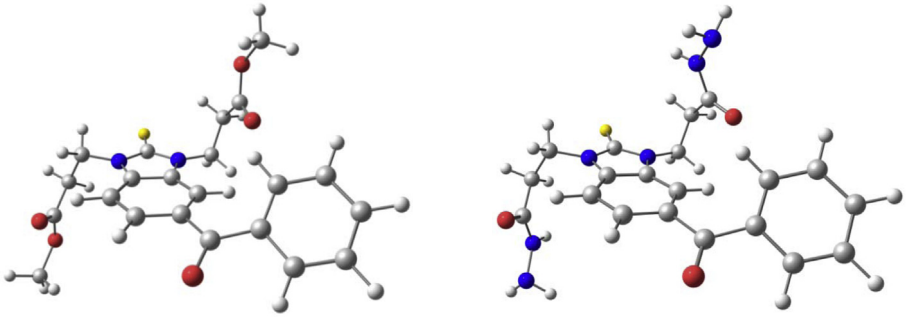

(a) (b)

Scheme 3 Optimized geometry of the most stable stereoisomer of **10** (a) and **15** (b).

the insignificant energy differences between the *cis* and *trans* conformers, the low energy requirements for the rotation of the benzoyl group and the additional factors affecting the crystal structure, the presence of different conformations in isolated state and in the crystal is not surprising. The crystal structure of **10** and the theoretically calculated geometry of the corresponding conformer are in an excellent agreement, with rmsd value of 0.3731 Å (Fig. S3c).

2.5. SAR

Based on the small energy differences between the different conformations, it was assumed that **10** might easily convert into its lowest-energy form in biologically relevant liquid medium. Therefore, the computational study on the possible mechanism of antioxidant action was carried out by using the global energy minimum conformations of **10** and **15**. UB3LYP/6-311 + + G** level of theory was applied in order to enable comparison with calculated reaction enthalpies of other well-known and structurally related radical scavengers.

A good antioxidant should be able to easily react with a wide variety of free radicals. This includes the HO•, which is the most reactive among the ROS with little selectivity toward the various possible sites of attack (Samuni et al., 1983); the less reactive HOO• capable of diffusing into remote cellular locations (Marnett, 1987) and responsible for the initiation of lipid peroxidation (Aikens and Dix, 1991); the alkoxyl radicals LO• which are formed from the reduction of peroxides and are less reactive than HO•, but significantly more reactive than the peroxyl radicals (León-Carmona and Galano, 2011); and the least reactive organic peroxyl radicals *i.e.* LOO• (Huie and Neta, 2002).

The studied benzimidazole-2-thiones partially resemble the structure of melatonin and its N-substituted derivatives (Phiphatwatcharaded et al., 2014) due to the presence of a flat conjugated aromatic heterocycle substituted at 5-position, as in melatonin, and side chains of approximately the same length containing carbonyl ester or amide function (Scheme 4).

Melatonin is known as a versatile antioxidant able to scavenge various free radicals (ROS and RNS) (Shirinzadeh et al., 2010). Its N-substituted derivatives exhibit *in vitro* antioxidant and anti-inflammatory activities. Hydrogen atom transfer (HAT) and single electron transfer (SET) were identified, from experimental data, as the main mechanisms for the reactions of melatonin, its N-substituted derivatives (Johns and Platts, 2014) and other indole derivatives (tryptophan and N-methylindole) with different free radicals (Solar et al., 1991):

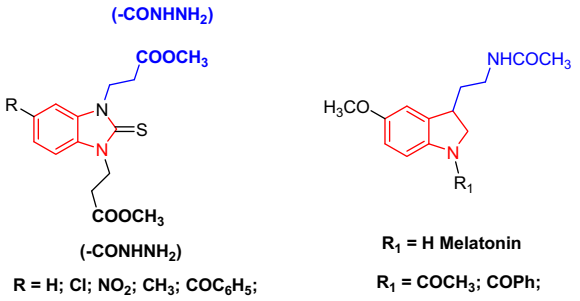

Scheme 4 Chemical structure of benzimidazole-2-thiones, melatonin and its N-substituted derivatives.

$$R{-}H + LOO^{\cdot} \rightarrow R^{\cdot} + LOOH \ (HAT)$$

$$R{-}H + LOO^{\cdot} \rightarrow RH^{+\cdot} + LOO^{-} \ (SET)/RH^{+\cdot} + LOO^{-} \rightarrow R^{\cdot} + LOOH \ (PT)$$

The SET mechanism for direct radical scavenging of melatonin is the most favorable mechanism in aqueous solution, while in nonpolar aprotic medium HAT is prevailing (Galano, 2011). Therefore, based on the structure similarities, these mechanisms are also expected to contribute to the overall free radical–scavenging activity of the benzimidazole-2-thiones studied by us.

The first mechanism to be considered was HAT. Lipid peroxidation inhibition is known to proceed by this mechanism and involves all aforementioned oxygen-based radicals (Klein et al., 2007; Frankel, 1998; Burton et al., 1985; De Heer et al., 2000). For effective lipid peroxidation inhibition, the radical formed by the antioxidant agent should be less reactive and more stable than the attacked LOO• i.e. the antioxidant should have lower bond dissociation enthalpy (BDE) than the free lipid radicals. The lower the BDE value, the higher the radical scavenging capacity of the antioxidant agent. For the accurate estimation of the antioxidant capacity via HAT by computational methods it is necessary to compare it to a lipid BDE value, representative for the chosen level of theory. In our study the lipid peroxyl and alkoxyl radicals were illustrated by the radicals of (Z)-4-hydroperoxyhex-2-ene, (Z)-4-hydroxyhex-2-ene, methyl hydroperoxide and methanol in gas-phase (Scheme 5).

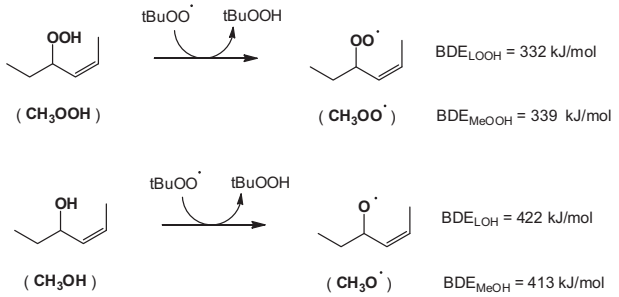

Scheme 5 BDE values of model lipid radicals calculated at B3LYP/6-311 + + G** level of theory.

Therefore, in order to scavenge the less reactive lipid peroxyl radicals, the antioxidant agents are expected to show BDE values below 330 kJ·mol^{-1}, while for scavenging of lipid alkoxyl radicals BDEs below 400 kJ·mol^{-1} are sufficient. The BDE values of $CH_3COO^{\cdot}$ and $CH_3O^{\cdot}$ show only small deviation from the two larger radicals, which is an indication that the reactivity of the lipid radicals is sufficiently well described even by the small methoxyl and methyl peroxyl radicals. Thus $CH_3COO^{\cdot}$ and $CH_3O^{\cdot}$ can be used in the following study of radical scavenging as reliable representation of the lipid radicals.

α-Tocopherol, which is an effective chain-breaking antioxidant, has BDE of 327 kJ/mol according to the calculations in gas-phase at B3LYP/6-311 + + G** level of theory (Klein et al., 2007). The O—H BDE values of quercetin range from 305 to 398 kJ·mol^{-1} (at the same computational scheme) as has been reported (Vagánek et al., 2012). Melatonin is able to donate a hydrogen atom from the methylene group next to the indolyl fragment with C—H BDE value of 319 kJ·mol^{-1} and from the indolyl N—H with BDE value of 322 kJ·mol^{-1} (calculated at B3LYP/6-31G(d,p) level of theory) (Velkov et al., 2009).

For the ester **10**, hydrogen atom abstraction would be possible from the alkyl groups in the side chains - the C—H bonds next to the benzimidazole N-atoms (*sites 1, 1′*, Fig. 4) or the C—H bonds next to the ester carbonyl groups (*sites 2, 2′*,

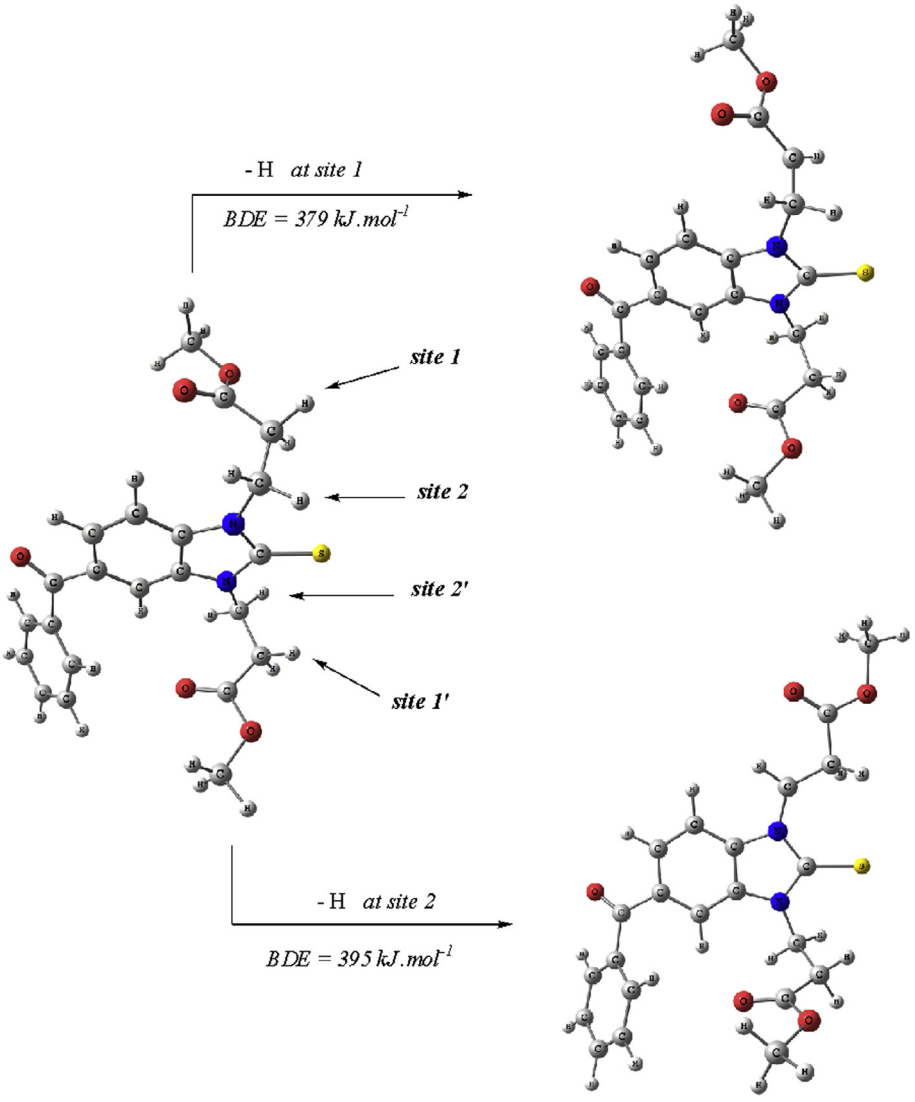

Figure 4 Hydrogen atom abstraction at different sites and corresponding B3LYP/6-311 + + G** bond dissociation enthalpies of 10 in kJ·mol^{-1}.

Fig. 4). After full geometry optimization of the resulting radical species, the BDEs related to each of these sites were calculated and compared. As could be seen from the values depicted in Fig. 4 the lipid radicals will attack preferentially the hydrogen atom of the C—H bond next to the carbonyl group. The corresponding BDE values are approximately 15 kJ·mol^{-1} lower than the BDE related to *sites 2* and *2′*. Obviously the proximity of the carbonyl groups and the lengthening of the C—H bonds due to the intramolecular C—H···S interactions considerably facilitate their cleavage. In comparison with the previously investigated 1,3-disubstituted-benzimidazol-2-imines (Mavrova et al., 2015) the methylene groups next to the N-atoms from the benzimidazole-2-thione ring are significantly less prone to donate a hydrogen atom.

Taking into account the estimated lipid BDE values, it can be concluded that **10** would be an efficient radical scavenger of lipid alkoxyl radicals but nor peroxyl radicals. Therefore, the protective effect of the ester benzimidazole-2-thiones against lipid peroxidation should be exerted by scavenging the highly reactive HO$^{\cdot}$, which initiates the degradation process, and the alkoxyl radicals LO$^{\cdot}$ formed from the reduction of lipid peroxides.

For the hydrazide derivatives, there are two more sites for hydrogen atom abstraction from each N-alkyl chain – from the amide N—H bond (*site 3*) and the amino N—H bonds (*site 4*) (Fig. 5). The BDE values for *site 1* and *2* in **15** are comparable to those in **10**. However, the N—H bonds in **15** show remarkably lower BDE values giving strong advantage to **15** as a radical scavenger as compared to **10**, where only C—H bonds could be cleaved. The most favorable site for the hydrogen atom abstraction is the amide N—H bond (*site 3*) with BDE of 308 kJ·mol^{-1}, close to the calculated BDE value for 4′—OH group of quercetin (Vagánek et al., 2012). The second preferred one is *site 4* with BDE of 345 kJ·mol^{-1}.

As the BDE value for *site 3* is lower than that of the lipid peroxyl radicals, **15** would be able to trap lipid peroxyl, as well as alkoxyl radicals, and inhibit directly the lipid peroxidation process. This makes the hydrazide benzimidazole-2-thiones more efficient lipid peroxidation inhibitors than the ester derivatives via HAT mechanism.

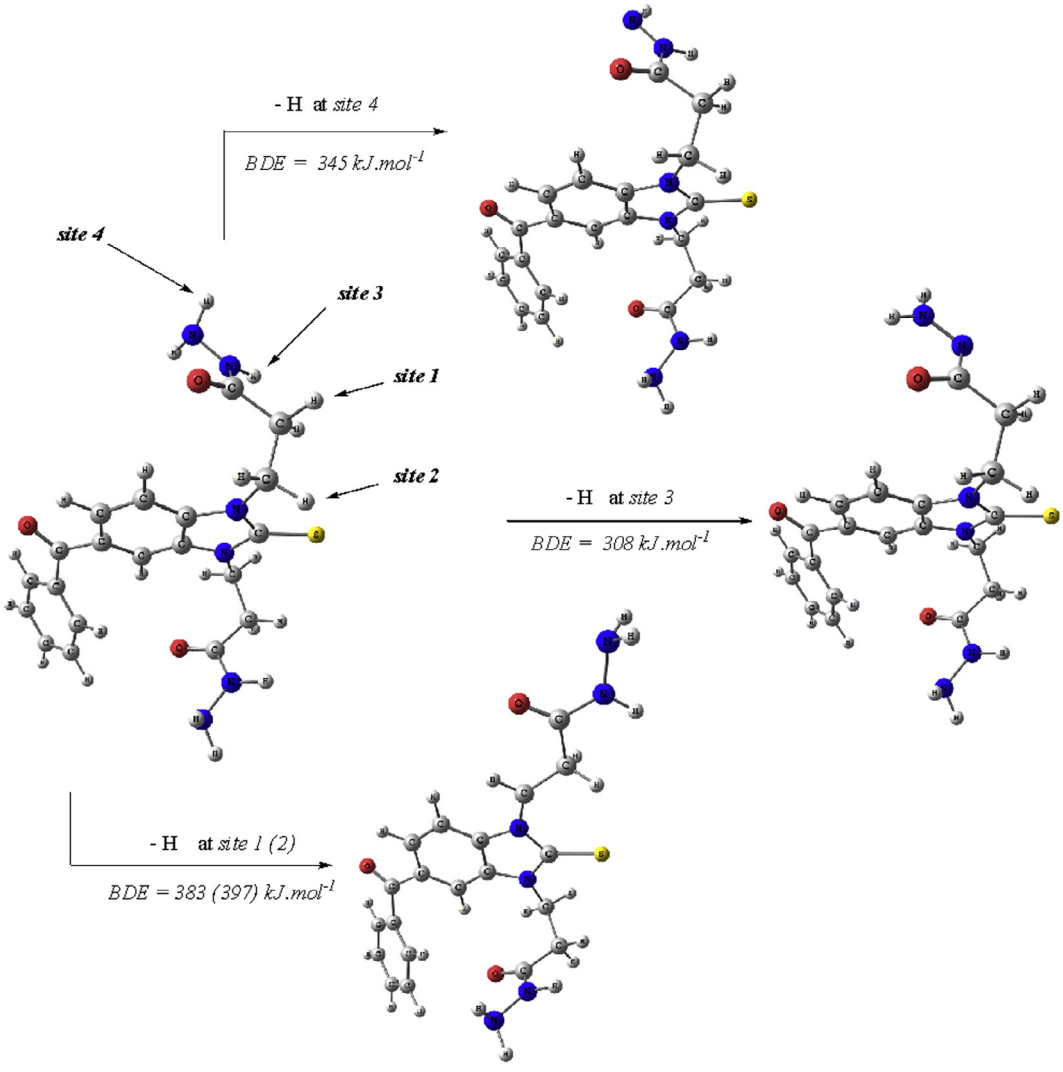

Figure 5 Hydrogen atom abstraction at different sites and corresponding B3LYP/6-311++G** bond dissociation enthalpies of **15** in kJ·mol^{-1}

In a polar aqueous medium, ionization mechanisms of antioxidant action, such as SET, are more likely to occur. SET is characterized by the ionization potential (IP) of the studied molecules and a lower IP implies an easier electron release. In order to estimate the probability **10** and **15** to react via the SET mechanism and compare their reactivity via this route, we optimized the geometry of their radical cations at B3LYP/6-311 + + G^{**} level of theory and calculated the corresponding IP values.

In gas state the IP value of **10** is found to be 691 kJ·mol^{-1} *i.e.* comparable to the value calculated for quercetin (698 kJ·mol^{-1}) by Vagánek et al. according to the same computational scheme (Vagánek et al., 2012). The hydrazide **15** showed IP of 682 kJ·mol^{-1}. In water, the solvation of the electron and the positively charged radical species lowers the IP values. For this reason, the IP and BDE values of **10** and **15** were calculated at IEF-PCM B3LYP/6-311 + + G^{**} level of theory and compared. The ester derivative **10** showed IP of 329 kJ·mol^{-1} in water, dropping below its water BDE (*site 1*) value 374 kJ·mol^{-1} and below the water IP of phenol - 346 kJ·mol^{-1}. Hydrazide **15** showed water IP of 328 kJ·mol^{-1}, while the water BDE value for hydrogen atom transfer from *site 3* was 320 kJ·mol^{-1}. Subsequently the SET mechanism of radical scavenging becomes preferred in water medium for **10**, and competitive to HAT for **15**.

The ability of a system to donate one electron can be estimated also by calculating the relaxed ionization potential (rIP) according to the approach suggested (Gazquez et al., 2007). Conformation changes in the side chain of melatonin are reported to have little impact on rIP (Johns and Platts, 2014), as the removal of an electron to the neutral molecule affects only the flat conjugated indole moiety. Thus rIP of 6.85 eV was computed at B3LYP/6-31 + G^{*} level of theory for melatonin in gas phase (Johns and Platts, 2014), which is in good accordance with the value estimated by photoelectron measurements (Cannington and Ham, 1983). The rIP values for **10** and **15** (computed in gas phase at B3LYP/6-311 + + G^{**} level of theory) are 7.14 and 7.04 eV, which suggest a good capacity for the benzimidazole-2-thiones to donate one electron and scavenge free radicals via the SET mechanism.

Therefore, the studied benzimidazole-2-thiones are expected to easily transfer an electron to the lipid radicals and form radical cations. After the transfer of the free electron, the melatonin can undergo molecular rearrangements and produce several metabolites, which in turn act as radical scavengers (Johns and Platts, 2014). In the present case several routes of radical scavenging also exist (Scheme 6).

The electron transfer might be immediately followed by proton transfer and complimented by the formation of a cyclic intermediate of the benzimidazole-2-thiones. The latter would be a neutral radical able to scavenge $CH_3COO^{\cdot}$ and $CH_3O^{\cdot}$ (adduct formation) and inhibit the lipid peroxidation. On the other hand, due to the substantial spin density localized over the S-atom in the radical cation, it is anticipated that another possible way would be to bind a lipid radical at this site and form a cation adduct.

A good antioxidant should be able to cross physiologic barriers and to be quickly transported into the cells. For this reason, the solubility of the studied compounds in lipids and water was assessed by calculating log P, molecular size, flexibility and the presence of hydrogen-donor and acceptors with a Molinspiration tool (Table 4) (Molinspiration Cheminformatics, 2015).

The $m_i$log P values of the benzimidazole-2-thione esters **6**–**10** and hydrazides **11**–**15** range between 0 and 2.7 outlining various possible biological sites where they can act as antioxidant agents. The lipophilicity of the esters **6**–**10** is slightly higher and they can be applied as lipid peroxidation protectors. As more hydrophilic compounds, the hydrazides **11**–**15** may protect against ROS damage in the aqueous medium along with the traditional protectors vitamin C, lipoic acid and aqueous antioxidant enzymes.

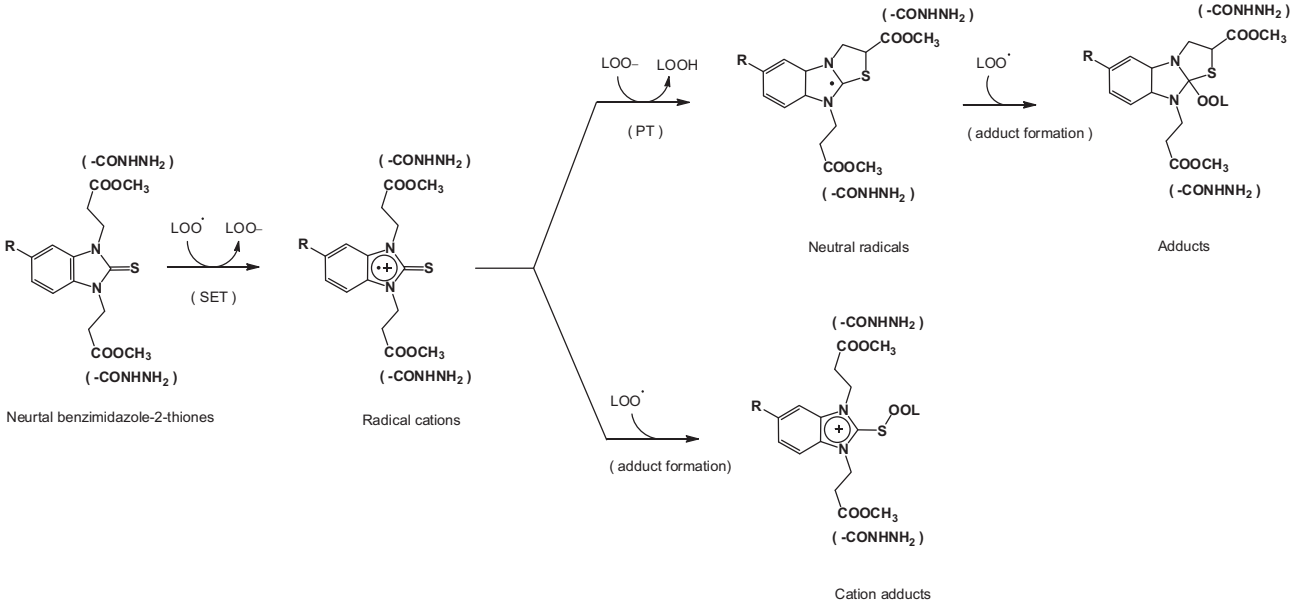

Scheme 6 Hypothetical mechanism of antioxidant action of benzimidazole-2-thiones via SET.

Table 4 Calculated physicochemical properties of compounds **6**–**15**.

No.	$m_i \log P$[a]	TPSA[b]	N_{atoms}[c]	MW[d]	N_{ON}[e]	N_{OHNH}[f]	$N_{viol.}$[g]	$N_{rotb.}$[h]	Vol[i]
6	1.20	62	22	322	6	0	0	8	282
7	1.62	62	23	336	6	0	0	8	300
8	1.14	108	25	367	9	0	0	9	306
9	1.85	62	23	357	6	6	0	8	296
10	2.63	79	30	427	7	0	0	10	390
11	0.27	109	20	290	6	6	1	6	261
12	0.70	109	21	304	6	6	1	6	277
13	0.21	155	23	335	1	7	1	7	284
14	0.93	109	21	325	6	6	1	6	274
15	1.70	127	28	395	7	6	1	8	351

[a] Octanol-water partition coefficient, calculated by the methodology developed by Molinspiration.
[b] Topological surface area.
[c] Number of nonhydrogen atoms.
[d] Molecular weight.
[e] Number of hydrogen-bond acceptors (O and N atoms).
[f] Number of hydrogen-bond donors (OH and NH groups).
[g] Number of "Rule of five" violations.
[h] Number of rotatable bonds.
[i] Molecular volume.

Table 5 Crystal data and most important structure refinement indicators for compounds **6** and **10**.

Compound reference	**6**	**10**
Chemical formula	$C_{15}H_{18}N_2O_4S$	$C_{22}H_{22}N_2O_5S$
Formula Mass	322.37	426.47
Crystal system	Triclinic	Monoclinic
Space group	*P-1*	$P2_1/n$
a/Å	8.6065(4)	12.1735(4)
b/Å	9.3848(3)	13.0933(5)
c/Å	9.9524(4)	13.1689(4)
α/°	93.517(3)	90
β/°	94.516(3)	95.518(3)
γ/°	91.839(3)	90
Unit cell volume/Å^3	799.30(5)	2089.30(12)
Temperature/K	290	290
No. of formula units per unit cell, Z	2	4
Radiation type	MoKα	MoKα
Absorption coefficient, μ/mm^{-1}	0.221	0.192
No. of reflections measured	11,468	12,750
No. of independent reflections	5199	4514
R_{int}	0.0282	0.0305
Final R_1 values ($I > 2\sigma(I)$)	0.0670	0.0501
Final $wR(F^2)$ values ($I > 2\sigma(I)$)	0.2001	0.1496
Final R_1 values (all data)	0.1126	0.0759
Final $wR(F^2)$ values (all data)	0.2357	0.1734
Goodness of fit on F^2	1.250	1.119

Overall the calculated TPSA, molecular weight, number of rotatable bonds and number of hydrogen-bond acceptors and donors indicate good solubility and permeability of the studied compounds. Having in mind their relatively low hepatotoxicity, it could be concluded that they possess favorable properties for application as radical scavengers and oxidative stress inhibitors.

3. Conclusion

A series of novel 1,3-disubstituted benzimidazole-2-thione derivatives were synthesized by a new method using for the first time *aza*-Michael addition. The hepatotoxicity and the antioxidant activity of the compounds were examined. The antioxidant properties of the compounds with the lowest toxicity were evaluated using oxidative stress induced by *tert*-butylhydroperoxide (*tert*-BOOH) on rat hepatocytes. In order to determine the structure and its influence on the biological properties DFT computations and X-ray crystallography analysis were performed. The mechanisms of the antioxidant action of the tested compounds in nonpolar (lipid) and polar (aqueous) medium were studied based on calculated reaction enthalpies of hydrogen atom abstraction (HAT mechanism) and single-electron transfer (SET mechanism). The ester **10** and the hydrazide **15**, which revealed the lowest cytotoxic effects on isolated rat hepatocytes, exhibited statistically significant cytoprotective and antioxidant effects similar to those of quercetin. Having in mind these findings, 1,3-disubstituted benzimidazole-2-thione moiety can be regarded as a promising scaffold for the development of new effective radical scavengers and oxidative stress inhibitors for the treatment of liver disorders. Redox imbalance in liver is the cause for alcoholic and nonalcoholic fatty liver disease, hepatic encephalopathy, liver fibroproliferative diseases and hepatitis C where the application of antioxidant therapeutic agents would be very beneficial. Having in mind the relation of the enzyme xanthine oxidase to the redox state of the liver cells, screening of the newly synthesized compounds as inhibitors of xanthine oxidase is regarded as a further step of the study.

4. Experimental

Melting points (mp) were determined using an Electrothermal AZ 9000 3MK4 apparatus and were uncorrected. IR spectra were recorded on a Bruker spectrophotometer as potassium bromide disks and ATR. ^{1}H and ^{13}C NMR spectra were recorded on a Bruker Avance II+ 250 MHz and a Bruker Avance II+ 600 MHz NMR instrument. The spectra are referred to the solvent signal. Chemical shifts are expressed in ppm and coupling constants in Hz. The precise assignment

of the ^{1}H and ^{13}C NMR spectra was accomplished by measurement of 2D homonuclear correlation (COSY), DEPT-135 and 2D inverse detected heteronuclear (C—H) correlation HSQC. The reactions were monitored by thin layer chromatography, which was performed on Merck pre-coated plates (silica gel. 60 F254, 0.25 mm) and was visualized by fluorescence quenching under UV light (254 nm).

The chemicals used in the pharmacological experiments were as follows: pentobarbital sodium (Sanofi, France), HEPES (Sigma Aldrich, Germany), NaCl (Merck, Germany), KCl (Merck), D-glucose (Merck), $NaHCO_3$ (Merck), KH_2PO_4 (Scharlau Chemie SA, Spain), $CaCl_2.2H_2O$ (Merck), $MgSO_4.7H_2O$ (Fluka AG, Germany), collagenase from *Clostridium histolyticum* type IV (Sigma Aldrich), albumin, bovine serum fraction V, minimum 98% (Sigma Aldrich), EGTA (Sigma Aldrich), 2-thiobarbituric acid (4,6-dihydroxy pyrimidine-2-thiol; TBA) (Sigma Aldrich), trichloroacetic acid (TCA) (Valerus, Bulgaria), 2,2′-dinitro-5,5′-dithiodibenzoic acid (DTNB) (Merck), lactate dehydrogenase (LDH) kit (Randox, UK), *tert*-butyl hydroperoxide (Sigma Aldrich), and carbon tetrachloride (Merck).

4.1. Synthesis of compounds ***1–5***

The starting 4-substituted-1,2-diaminobenzenes were commercially available. The 5-substituted benzimidazole-2-thiols **1–5** were synthesized as previously reported (Mavrova et al., 2005a,b).

4.2. General procedure for preparation of compounds ***6–10***

To a solution of 5-substituted-2-mercaptobenzimidazole (0.01 mol) in DMF (20 ml) methyl acrylate (0.02 mol) was added and the mixture was boiled under reflux for 2–5 h. The reaction was monitored by TLC and after finishing the reaction the DMF was distilled off under vacuum and a small portion of methanol was added to the residue. It was left over night. The crude crystals were recrystallized from methanol.

*4.2.1. Methyl 3-[3-(3-methoxy-3-oxopropyl)-2-thioxo-2,3-dihydro-1H-benzimidazol-1-yl]propanoate (**6**)*

White needle shaped crystals (4.2 g, 65% yield), mp 70–72 °C (from methanol). IR (ν_{max}/cm^{-1}) 3071, 3039 (ν CH arom), (2952 (ν_{as} CH_3), 2850 (ν_s CH_3), 1731 (ν C═O), 1161 (ν COC), 1123 (ν C═S). ^{1}H NMR (250 MHz, DMSO-d_6) δ (ppm) 7.53–7.50 (dd, J = 3.2 Hz, J = 5.8 Hz 1H, Ar—H), 7.29–7.25 (dd, J = 3.1 Hz, J = 6.0 Hz, 1H, Ar—H), 4.55–4.49 (t, J = 7.3 Hz, J = 14.5 Hz, 4H, CH_2), 3.57 (s, 6H, CH_3), 2.89–2.74 (t, J = 7.2 Hz, J = 14.3 Hz, 4H, CH_2). ^{13}C NMR (62 MHz, DMSO-d_6) δ 171.0, 168.1, 131.2, 122.8, 109.8, 51.5, 39.9, 31.6.

4.2.2. Methyl 3-[3-(3-methoxy-3-oxopropyl)-5-methyl-2-thioxo-2,3-dihydro-1H-benzimidazol-1-yl]propanoate ***(7)***

White crystals (3.9 g, 67% yield), mp 91–93 °C (from methanol). IR (ν_{max}/cm^{-1}) 2950 (ν_{as} CH_3), 2848 (ν_s CH_3), 1720 (ν C═O), 1171 (ν COC), 1140 (ν C═S). ^{1}H NMR (600 MHz, DMSO-d_6) δ (ppm) 7.21–7.20 (d, J = 8.3 Hz 1H, Ar—H), 7.11 (s, 1H, Ar—H), 7.08–7.06 (d, J = 8.2 Hz, 1H, Ar—H), 4.58–4.54 (td, J = 2.2 Hz, J = 14.2 Hz, 4H, CH_2), 3.69–3.66 (d, J = 12.0 Hz, 6H, CH_3) 2.94–2.90 (dt, J = 7.4 Hz, J = 14.2 Hz, 4H, CH_2), 2.46 (s, 3H, CH_3). ^{13}C NMR (150 MHz, DMSO-d_6) δ 171.7, 171.6, 168.6, 133.3, 131.9, 129.8, 124.1, 109.6, 109.1, 51.9, 40.4, 40.3, 32.1, 21.6.

4.2.3. Methyl 3-[3-(3-methoxy-3-oxopropyl)-5-nitro-2-thioxo-2,3-dihydro-1H-benzimidazol-1-yl]propanoate ***(8)***

Yellow needle shaped crystals (2.5 g, 62% yield), mp 94–96 °C (from methanol). IR (ν_{max}/cm^{-1}) 2954 (ν_{as} CH_3), 2843 (ν_s CH_3), 1728 (ν C═O), 1518 (ν_{as} NO_2), 1340 (ν_s NO_2), 1174 (ν COC), 1186 (ν C═S). ^{1}H NMR: (600 MHz, DMSO) δ (ppm) 8.58 (s, 2H, Ar—H), 8.10–8.08 (dd, J = 2.2 Hz, J = 8.9 Hz, 2H, Ar—H), 7.82–7.81 (d, J = 8.9 Hz, 1H, Ar—H), 4.64–4.62 (t, J = 6.7 Hz, J = 13.4 Hz, 4H, CH_2), 3.56 (s, 6H, CH_3), 2.98–2.96 (t, J = 6.5 Hz, J = 13.4 Hz, 4H, CH_2). ^{13}C NMR (150 MHz, DMSO-d_6) δ 171.7, 171.6, 149.9, 148.2, 143.3, 133.5, 120.1, 117.6, 108.4, 52.0, 40.9, 34.3.

*4.2.4. Methyl 3-[3-(3-methoxy-3-oxopropyl)-5-chloro-2-thioxo-2,3-dihydro-1H-benzimidazol-1-yl]propanoate (**9**)*

White crystals (2.6 g, 60% yield), mp 98–100 °C (from methanol). IR (ν_{max}/cm^{-1}) 2951 (ν_{as} CH3), 2835 (ν_s CH3), 1720 (ν C═O); 1261, 1170 (ν COC), 1134 (ν C═S). ^{1}H NMR (250 MHz, DMSO-d_6) δ (ppm) 7.72–7.71 (d, J = 1.85 Hz, 1H, Ar—H), 7.55–7.52 (d, 1H, J = 8.6 Hz, Ar—H), 7.33–7.29 (dd, J = 1.9 Hz, J = 8.7 Hz, 1H, Ar—H), 4.52–4.46 (t, J = 7.2 Hz, J = 14.2 Hz, 4H, CH_2), 3.58–3.56, (d, J = 3.20 Hz, 6H, CH_3), 2.85–2.80 (t, J = 7.2 Hz, J = 14.2 Hz, 4H, CH_2). ^{13}C NMR (62 MHz, DMSO-d_6) δ 171.0, 170.9, 168.9, 132.2, 130.2, 127.4, 122.6, 111.0, 110.0, 51.6, 51.5, 40.1, 31.4, 31.3.

*4.2.5. Methyl 3-[3-(3-methoxy-3-oxopropyl)-5-benzoyl-2-thioxo-2,3-dihydro-1H-benzimidazol-1-yl]propanoate (**10**)*

Yellow crystals (0.93, 62%), mp 100–101 °C(from methanol). IR (ν_{max}/cm^{-1}) 1738 (ν C═O), 1641 (ν C═O), 1124 (ν C═S), 1261, 1169 (ν COC). ^{1}H NMR (250 MHz, DMSO-d_6) δ (ppm) 7.94 (s, 1H, Ar—H), 7.80–7.76 (m, 2H, Ar—H), 7.73–7.69 (dt, J = 2.3 Hz, J = 7.2 Hz, 1H, Ar—H), 7.67–7.66 (m, 2H, Ar—H), 7.62–7.55 (m, 1H, Ar—H), 7.59–7.55 (t, J = 1.4 Hz, J = 3.0 Hz, 1H, Ar—H), 4.60–4.52 (dt, J = 7.1 Hz, J = 13.8 Hz, 4H, CH_2), 2.90–2.83 (d, J = 6.3 Hz, 6H, CH_3) 2.90–2.83 (dt, J = 6.8 Hz, J = 13.9 Hz, 4H, CH_2). ^{13}C NMR (62 MHz, DMSO-d_6) δ 194.9, 171.0, 170.9, 169.9, 137.4, 134.5, 132.5, 131.6, 131.3, 129.6, 128.5, 125.5, 111.3, 109.5, 51.6, 51.5, 40.2, 31.5.

4.3. General procedure for preparation of compounds ***11–15***

Hydrazine hydrate (0.04 mol) and 0.01 mol of the corresponding 1,3-disubstituted-2-thione benzimidazole esters **6–10** were refluxed in absolute ethanol for 2 h. After completion of reaction the mixture was cooled and the obtained crystals were filtered off and recrystallized with ethanol.

*4.3.1. 1,3-bis[3-(hydrazinooxy)-3-oxopropyl]-1,3-dihydro-2H-benzimidazole-2-thione (**11**)*

White powder (3.4 g, 77% yield), mp 220–222 °C (from ethanol). IR (ν_{max}/cm^{-1}) 3293 (νN—H), 1638 (ν C═O), 1607 (δ NH 2), 1531 (δ N—H), 1119 (ν C═S). ^{1}H NMR (250 MHz,

DMSO-d_6) δ (ppm) 9.10 (s, 2H, NH), 7.49–7.45 (dd, J = 3.18 Hz, J = 5.9 Hz, 2H, Ar—H), 7.27–7.23 (dd, J = 3.12 Hz, J = 6.0 Hz, 2H, Ar—H),4.50–4.45 (t, J = 6.8 Hz, J = 14.4 Hz, 4H, CH_2), 4.17 (s, 4H, NH_2), 2.57–2.51 (m, 4H, CH_2). ^{13}C NMR (62 MHz, DMSO-d_6) δ 168.9, 168.0, 131.3, 122.7, 109.8, 40.7, 31.6.

*4.3.2. 1,3-bis[3-(hydrazinooxy)-3-oxopropyl]-5-methyl-1,3-dihydro-2H-benzimidazole-2-thione (**12**)*

White powder (625 mg, 77% yield), mp 211–213° (from ethanol). IR (ν_{max}/cm^{-1}) 3290 (νN—H), 1640 (ν C═O), 1603 (δ NH 2), 1529 (δ N—H), 1134 (ν C═S). ^{1}H NMR (600 MHz, DMSO-d_6) δ (ppm) 9.23–9.22 (d, J = 10.0 Hz, 2H, NH), 7.44–7.43 (d, J = 8.07 Hz, 1H, Ar—H), 7.39 (s, 1H, Ar—H), 7.17–7.16 (m, J = 8.3 Hz, 1H, Ar—H), 4.54–4.51 (m, J = 14.6 Hz, 4H, CH_2), 4.31 (s, 4H, NH_2), 2.62–2.60 (m, 4H, CH_2), 2.49 (s, 3H, CH_3). ^{13}C NMR (62 MHz, DMSO-d_6) δ 168.9, 169.8, 167.7, 132.3, 131.4, 129.4, 123.6, 109.8, 109.4, 40.7, 40.6, 31.7, 31.6, 21,0.

*4.3.3. 1,3-bis[3-(hydrazinooxy)-3-oxopropyl]-5-nitro-1,3-dihydro-2H-benzimidazole-2-thione (**13**)*

Yellow powder (400 mg, 75% yield), mp 230–232 °C (from ethanol). IR (ν_{max}/cm^{-1}) 3309 (νN—H), 1637 (ν C═O), 1607 (δ NH 2), 1533 (δ N—H), 1150 (ν C═S). ^{1}H NMR (600 MHz, DMSO-d_6) δ (ppm) 9.11–9.10 (d, J = 4.9 Hz, 2H, NH), 8.41–8.40 (d, J = 2.1 Hz, 2H, Ar—H), 8.18–8.16 (dd, J = 2.2 Hz, J = 8.9 Hz, 1H, Ar—H), 7.64–7.63 (d, J = 8.8 Hz, 1H, Ar—H), 4.54–4.49 (dt, J = 6.8 Hz, J = 15.5 Hz, 4H, CH_2), 4.23 (s, 4H, NH_2), 2.59–2.56 (dt, J = 6.8 Hz, J = 4.8 Hz, 4H, CH_2). ^{13}C NMR (150 MHz, DMSO-d_6) δ 171.6, 169.3, 169.2, 143.3, 136.5, 131.8, 119.4, 110.4, 106.4, 41.7, 41.6, 31.9, 31.8.

*4.3.4. 1,3-bis[3-(hydrazinooxy)-3-oxopropyl]-5-chloro-1,3-dihydro-2H-benzimidazole-2-thione (**14**)*

Pale beige powder (600 mg, 64% yield), mp 205–207 °C (from ethanol). IR (ν_{max}/cm^{-1}) 3302 (νN—H), 1642 (ν C═O), 1608 (δ NH 2), 1534 (δ N—H), 1133 (ν C═S). ^{1}H NMR (600 MHz, DMSO-d_6) δ (ppm) 9.09–9.08 (d, J = 8.4 Hz, 2H, NH), 7.63–7.62 (d, J = 2.1 Hz, 2H, Ar—H), 7.46–7.44 (d, J = 8.5 Hz, 1H, Ar—H), 7.28–7.27 (dd, J = 2.0 Hz, J = 8.6 Hz, 1H, Ar—H), 4.45–4.42 (dt, J = 7.3 Hz, J = 13.8 Hz, 4H, CH_2), 4.17 (s, 4H, NH_2), 2.54–2.50 (m, 4H, CH_2). ^{13}C NMR (75 MHz, DMSO-d_6) δ: 169.4, 169.3, 168.1, 132.8, 131.8, 129.8, 124.1, 110.3, 109.9, 41.1, 41.0, 32.1, 32.0.

*4.3.5. 1,3-bis[3-(hydrazinooxy)-3-oxopropyl]-5-benzoyl-1,3-dihydro-2H-benzimidazole-2-thione (**15**)*

White powder (750 mg, 67% yield), mp 128–130 °C (from ethanol). IR (ν_{max}/cm^{-1}) 3305 (νN—H), 1647 (ν C═O), 1600 (δ NH 2), 1631 (ν C═O), 1531 (δ N—H), 1120 (ν C═S). ^{1}H NMR (600 MHz, DMSO-d_6) δ (ppm) 9.12–9.11(d, J = 5.8 Hz, 2H, NH), 8.11 (s, 1H, Ar—H), 7.78–7.77 (d, J = 7.2 Hz, 2H, Ar—H), 7.70–7.68 (t, J = 7.4 Hz, J = 14.8 Hz, 1H, Ar—H), 7.65–7.63 (dd, J = 1.2 Hz, J = 8.3 Hz, 1H, Ar—H), 7.60–7.59 (d, J = 2.5 Hz, 1H, Ar—H), 7.58–7.57 (d, J = 7.6 Hz, 2H, Ar—H), 4.51–4.47 (dt, J = 6.9 Hz, J = 13.8 Hz, 4H, CH_2), 4.24 (s, 4H, NH_2), 2.57–2.55 (t, J = 6.6 Hz, J = 13.3 Hz, 4H, CH_2). ^{13}C NMR (150 MHz, DMSO-d_6) δ 195.4, 170.4, 169.3, 137.8, 135.0, 133.0, 131.9, 131.8, 130.2, 129.0, 125.9, 111.9, 110.0, 79.6, 41.5, 41.4, 32.0. 31.9.

4.4. Hepatotoxicity assay

4.4.1. Animals

The experiments were carried out on male Wistar rats (body weight 200–250 g). The rats were housed in plexiglass cages (3 per cage) in a 12/12 light/dark cycle, under standard laboratory conditions (ambient temperature 20 °C ± 2 °C and humidity 72% ± 4%) with free access to water and standard pelleted rat food 53-3, produced according to ISO 9001:2008.

Animals were purchased from the National Breeding Center, Sofia, Bulgaria. At least 7 days of acclimatization were allowed before the commencement of the study. The health of the animals was monitored regularly by a veterinary physician. The vivarium (certificate of registration of farm no. 0072/01.08.2007) was inspected by the Bulgarian Drug Agency in order to check the husbandry conditions (no. A-11-1081/03.11.2011). All performed procedures were approved by the Institutional Animal Care Committee and the principles stated in the European Convention for the Protection of Vertebrate Animals used for Experimental and other Scientific Purposes (ETS 123) Council of Europe (1991), and were strictly followed throughout the experiment.

4.4.2. Experimental design

4.4.2.1. Isolation and incubation of hepatocytes. The rats were anesthetized with sodium pentobarbital (0.2 ml/100 g). An optimized *in situ* liver perfusion using less reagents and shorter time of cell isolation was performed. The method provided a high amount of live and metabolically active hepatocytes (Mitcheva et al., 2006).

After portal catheterization, the liver was perfused with HEPES buffer (pH = 7.85) + 0.6 mM EDTA (pH = 7.85), followed by clean HEPES buffer (pH = 7.85) and finally HEPES buffer containing collagenase type IV (50 mg/200 ml) and 7 mM $CaCl_2$ (pH = 7.85). The liver was excised and minced into small pieces, and hepatocytes were dispersed in Krebs–Ringer-bicarbonate (KRB) buffer (pH = 7.35) + 1% bovine serum albumin.

Cells were counted under the microscope and the viability was assessed by Trypan blue exclusion (0.05%) (Fau et al., 1992). Initial viability averaged 89%.

Cells were diluted with KRB to make a suspension of about 3×10^6 hepatocytes/ml. Incubations were carried out in flasks containing 3 ml of the cell suspension (i.e. 9×10^6 hepatocytes) and were performed in a 5% CO_2 + 95% O_2 atmosphere.

Cells were incubated with concentration 250 μM from the compounds and 75 μM *tert*-butyl hydroperoxide (Mavrova et al., 2005b; Takayama et al., 2001).

4.4.3. Biochemical assays

4.4.3.1. Lactate dehydrogenase (LDH) release. After incubation, the hepatocytes were centrifuged for 4 min at 500 rpm and the supernatant was used for measuring LDH release spectrophotometrically by LDH kit (Fau et al., 1994).

4.4.3.2. Reduced glutathione (GSH) depletion. At the end of the incubation, isolated rat hepatocytes were centrifuged (at

4 °C) and the pellet was used for evaluating the level of intracellular GSH. It was assessed by measuring non-protein sulfhydryls after precipitation of proteins with trichloroacetic acid (TCA), followed by measurement of thiols in the supernatant with DTNB. The absorbance was measured at 412 nm (Fau et al., 1992).

4.4.3.3. Malondialdehyde (MDA) assay. After incubation, 1 ml from the hepatocyte suspension was taken and added to 0.67 ml of 20% (w/v) TCA. After centrifugation, 1 ml of the supernatant was added to 0.33 ml of 0.67% (w/v) 2-thiobarbituric acid (TBA) and heated at 100 °C for 30 min. The absorbance was measured at 535 nm, and the amount of TBA-reactants was calculated using a molar extinction coefficient of MDA $1.56 \times 10^5\ M^{-1}\ cm^{-1}$ (Fau et al.,1992).

4.4.4. Statistical analysis

For statistical analysis of the data, we used the statistical program 'MEDCALC'. Results are expressed as mean ± SEM for 6 experiments. The significance of the data was assessed using the nonparametric Mann–Whitney test. A level of $P < 0.05$ was considered significant. Three parallel samples were used.

4.5. X-ray experimental

Single crystals (colorless blocks with approximate dimensions $0.25 \times 0.22 \times 0.2\ mm^3$) of **6** and **10** were obtained by slow evaporation from methanol. A transparent and crack free crystal was carefully selected and mounted on a glass capillary. Diffraction data were collected at room temperature by ω-scan technique, on an Agilent Diffraction SuperNova Dual four-circle diffractometer equipped with Atlas CCD detector using mirror-monochromatized MoKα radiation from a micro-focus source ($\lambda = 0.7107$ Å). The determination of cell parameters, data integration, scaling and absorption correction was carried out using the CrysAlis Pro program package (CrysAlis PRO, 2011). The structures were solved by direct methods (SHELXS-2014) (Sheldrick, 2008) and refined by full-matrix least-square procedures on F^2 (SHELXL-2014). The heavy atoms (C, N, O and S) were positioned from difference Fourier maps while hydrogen atoms were placed at idealized positions. The non-hydrogen atoms were refined anisotropically while the hydrogen atoms were constrained to ride on their parent atom with U_{iso}(H) values of $1.2U_{eq}$ (C). A summary of the fundamental crystal and refinement data is provided in Table 5. Crystallographic data (excluding structure factors) for the structural analysis have been deposited with the Cambridge Crystallographic Data Centre, Nos. CCDC-1496636 (**6**) and CCDC-1496637 (**10**). Copies of this information may be obtained free of charge from The Director, CCDC, 12 Union Road, Cambridge, CB2 1EZ, UK. Fax: +44 (1223)336-033, e-mail: deposit@ccdc.cam.ac.uk, or www.ccdc.cam.ac.uk.

4.6. Computational details

All theoretical calculations were performed using the Gaussian 09 package (Frisch et al., 2009) of programs. Geometry and vibrational frequencies of species studied were performed by an analytical gradient technique without any symmetry constraint. All the results were obtained using the density functional theory (DFT), employing the B3LYP (Becke's three-parameter non-local exchange (Becke, 1993; Lee et al., 1988 correlation potentials). Natural bond orbitals (NBO) analysis (Reed et al., 1988; Carpenter and Weinhold, 1988; Weinhold and Carpenter, 1988) has been performed to characterize the delocalization of electron density within the molecule.

The equations used for calculation of dissociation enthalpy (BDE) and ionization potential (IP) of the studied compounds are given below:

$$BDE = H(R^{\cdot}) + H(H^{\cdot}) - H(R{-}H)$$

$$IP = H(R^{\cdot+}) + H(e^{-}) - H(R{-}H)$$

The enthalpy of the hydrogen atom, H(H) was obtained by the same method and basis set. All reaction enthalpies were calculated at 298 K. The enthalpies of proton $H(H^+)$, and electron, $H(e^-)$, were taken from the literature: 6.197 kJ/mol and 3.145 kJ/mol, respectively (Klein et al., 2007). Solvation enthalpies of proton H(H+), electron, $H(e^-)$, in water, determined using IEF-PCM DFT/B3LYP/6-311++G** calculations, were used as reported (Rimarčík et al., 2010). The lipid radical was modeled for comparison according to the same computational scheme.

Relaxed IP was calculated as the difference between the energy of the optimized radical cation and the optimized neutral molecule. (Johns and Platts, 2014).

Acknowledgments

The financial support of this work by the National Science Fund of Bulgaria (Contracts RNF01/0110) is gratefully acknowledged.

Appendix A. Supplementary material

Supplementary data associated with this article can be found, in the online version, at http://dx.doi.org/10.1016/j.arabjc.2016.12.003.

References

Achar, K., Hosamani, K., Seetharamareddy, H., 2010. *In-vivo* analgesic and anti-inflammatory activities of newly synthesized benzimidazole derivatives. Eur. J. Med. Chem. 45, 2048–2054.

Aikens, J., Dix, T.A., 1991. Perhydroxyl radical (HOO·) initiated lipid peroxidation. The role of fatty acid hydroperoxides. J. Biol. Chem. 266, 15091–15098.

Alasmary, F., Snelling, A., Zain, M., Alafeefy, A., Awaad, A., Karodia, N., 2015. Synthesis and evaluation of selected benzimidazole derivatives as potential antimicrobial agents. Molecules 20, 15206–15223.

Arora, R., Kaur, N., Bansal, Y., Bansal, G., 2014. Novel coumarin–benzimidazole derivatives as antioxidants and safer anti-inflammatory agents. Acta Pharm. Sin. B 4, 368–375.

Ayhan-Kilcigil, G., Kuş, C., Çoban, T., Özdamar, E., Can-Eke, B., 2014. Identification of a novel series of N-phenyl-5-[(2-phenylbenzimidazol-1-yl)methyl]-1,3,4-oxadiazol-2-amines as potent antioxidants and radical scavengers. Arch. Pharm. (Weinheim, Ger.) 347, 276–282.

Basu, B., Mandal, B., 2015. Green synthetic approaches for biologically relevant heterocycles. In: Brahmachari, G. (Ed.), Sustainable Synthesis of Benzimidazoles, Quinoxalines, and Congeners. Elsevier, Amsterdam, pp. 209–256.

Becke, A.D.J., 1993. Density functional thermochemistry. III. The role of exact exchange. J. Chem. Phys. 98, 5648–5652.

Bespalov, A.Y., Gorchakova, T.L., Ivanov, A.Y., Kuznetsov, M.A., Kuznetsova, L.M., Pankova, A.S., Prokopenko, L.I., Avdontceva, M.S., 2015. Alkylation and aminomethylation of 1,3-dihydro-2H-benzimidazole-2-thione. Chem. Heterocycl. Comp. 50, 1547–1558.

Blaauboer, B., Boobis, A.R., Castell, J.V., Coecke, S., Groothuis, G. M., Guillouzo, M., et al, 1994. Practical applicability of hepatocyte cultures in routine testing: the report and recommendations of ECVAM Workshop 1. ATLA. Altern. Lab. Anim. 22, 231.

Burton, G.W., Doba, T., Gabe, E.J., Hughes, L., Lee, F.L., Prasad, L., Ingold, K.U., 1985. Autoxidation of biological molecules. Maximizing the antioxidant activity of phenols. J. Am. Chem. Soc. 107, 7053–7065.

Cannington, P.H., Ham, N.S, 1983. J. Electron Spectrosc. Relat. Phenom. 32, 139.

Carpenter, J.E., Weinhold, F., 1988. J. Mol. Struct. (Theochem) 46, 41–62.

Cooke, M., Evans, M., Dizdaroglu, M., 2003. Oxidative DNA damage: mechanisms, mutation, and disease. J. Lunec, FASEB J. 17, 1195–1214.

Council of Europe. European Convention for the Protection of Vertebrate Animals used for Experimental and other Scientific Purposes. CETS no. 123, 1991 [displayed 30 May 2007]. Available at: <http://conventions.coe.int/treaty/Commun/QueVoulezVous.asp?NT=123ECL=ENG>.

Cox, P.J., Kechagias, D., Kelly, O., 2008. Conformations of substituted benzophenones. Acta Cryst. B 64, 206–216.

CrysAlis PRO, 2001. Agilent Technologies. UK Ltd, Yarnton, England.

De Heer, M.I., Mulder, P., Korth, H., Ingold, K.U., Lusztyk, J., 2000. Hydrogen atom abstraction kinetics from intramolecularly hydrogen bonded ubiquinol-0 and other (poly)methoxy phenols. J. Am. Chem. Soc. 122, 2355–2360.

El Ashry, E.S.H., Kilany, Y.E., Nahas, N.M., Barakat, A., Al-Qurashi, N., Ghabbour, H.A., Fun, H.-K., 2016. Synthesis and crystal structures of benzimidazole-2-thione derivatives by alkylation reactions. Molecules 21, 12–23.

Frankel, E.N., 1998. Lipid oxidation. The Oily Press, Dundee, Scotland.

Farmanzadeh, D., Najafi, M., 2015. Theoretical study of anticancer properties of indolyl-oxazole drugs and their interactions with DNA base pairs in gas phase and solvent. J. Theor. Comput. Chem. 26, 831–844.

Fau, D., Berson, A., Eugene, D., Fromenty, B., Fisch, C., Pessayre, D., 1992. Mechanism for the hepatotoxicity of the antiandrogen, nilutamide. Evidence suggesting that redox cycling of this nitroaromatic drug leads to oxidative stress in isolated hepatocytes. J. Pharmacol. Exp. Ther. 263, 69–77.

Fau, D., Eugene, D., Berson, A., Letteron, P., Fromenty, B., Fisch, C., Pessayre, D., 1994. Toxicity of the antiandrogen flutamide in isolated rat hepatocytes. J. Pharmacol. Exp. Ther. 269, 1–9.

Frisch, M.J., Trucks, G.W., Schlegel, H.B., et al., 2009. Gaussian 09, Revision A.1. Gaussian Inc., Wallingford CT.

Galano, A., 2001. On the direct scavenging activity of melatonin towards hydroxyl and a series of peroxyl radicals. Phys. Chem. Chem. Phys. 13, 7147–7157.

Galano, A., Tan, D., Reiter, R., 2011. Melatonin as a natural ally against oxidative stress: a physicochemical examination. J. Pineal Res. 51, 1–16.

Gazquez, J.L., Cedillo, A., Vela, A., 2007. J. Phys. Chem. A 111, 1966–1970.

Grimmet, M., 1997. Imidazole and benzimidazole synthesis. In: Katrizky, A.R., Meth-Cohn, O., Rees, C.W. (Eds.), Synthesis of Specifically Substituted Imidazoles and Benzimidazoles. first ed. Academic Press, New York, pp. 227–248.

Gurer-Orhan, H., Orhan, H., Suzen, S., Püsküllü, M.O., Buyukbingol, E., 2006. Synthesis and evaluation of in vitro antioxidant capacities of some benzimidazole derivatives. J. Enzyme Inhib. Med. Chem. 2, 241–247.

Hahn, F.E., Fehren, T.V., Lügger, T., 2005. The palladium complexes of a C3-bridged di(benzimidazol-2-ylidene) ligand via cleavage of a dibenzotetraazafulvalene. Inorg. Chim. Acta 35, 4137–4144.

Halliwell, B., 2006. Oxidative stress and neurodegeneration: where are we now? J. Neurochem. 97, 1634–1658.

Harti, J., Doudach, L., Faouzi, M., Taoufik, J., Ansar, M., 2014. Synthesis and antioxidant activity of some albendazole derivatives. J. Chem. Pharm. Res. 6, 781.

Huang, S., Hsei, I., Chen, C., 2006. Synthesis and anticancer evaluation of bis(benzimidazoles), bis(benzoxazoles), and benzothiazoles. Bioorg. Med. Chem. 14, 6106–6119.

Huie, R.E., Neta, P., 2002. Reactive oxygen species in biological systems: an interdisciplinary approach. In: Gilbert, D.L., Colton, C.A., Kluwer (Eds.), Chemistry of Reactive Oxygen Species. Academic Publishers, New York/Boston/Dordrecht/London/Moscow, pp. 33–63.

Ito, Y., Matsuura, T., Tabata, K., Ji-Ben, M., Fukuyama, K., Sasaki, M., Okada, S., 1987. Solid state photochemistry of methyl-substituted benzophenones. Tetrahedron 43, 1307–1312.

Jishkariani, D., Hall, C.D., Oliferenko, A., Tomlin, B.J., Steel, P.J., Katritzky, A.R., 2013. Thermal fragmentation of spirodithiohydantoins: a novel route to NHCs. RSC Adv. 3, 1669–1672.

Johns, J.R., Platts, J.A., 2014. Theoretical insight into the antioxidant properties of melatonin and derivatives. Org. Biomol. Chem. 12, 7820–7827.

Kamil, A., Akhtar, S., Noureen, S., Saify, Z.S., Jahan, S., Khan, K. M., Rahim, F., Taha, M., Mushtaq, N., Arif, M., Perveen, S., Chaudhary, M.I., 2015. 2-(2'-Pyridyl) benzimidazole analogs and their ß-glucuronidase inhibitory activity. J. Chem. Soc. Pak. 37, 787–791.

Karayel, A., Özbey, S., Ayhan-Kılcıgil, G., Kuş, C., 2015. Crystal structures and intermolecular interactions of two novel antioxidant triazolyl-benzimidazole compounds. Crystallogr. Rep. 60, 1084–1088.

Klein, E., Lukes, V., Ilcin, M., 2007. DFT/B3LYP study of tocopherols and chromans antioxidant action energetics. Chem. Phys. 336, 51.

Kuş, C., Ayhan-Kilcigil, G., Can Eke, B., iŞcan, M., 2004. Synthesis and antioxidant properties of some novel benzimidazole derivatives on lipid peroxidation in the rat liver. Arch. Pharmacal Res. 27, 156–163.

Kuş, C., Ayhan-Kılcıgil, G., Özbey, S., Kaynak, F., Kaya, M., Çoban, T., Can-Eke, B., 2008. Synthesis and antioxidant properties of novel N-methyl-1,3,4-thiadiazol-2-amine and 4–methyl-2H-1,2,4-triazole-3(4H)-thione derivatives of benzimidazole class. Bioorg. Med. Chem. 16, 4294–4303.

Kuş, C., Sözüdönmeza, F., Can-Ekeb, B., Çobanb, T., 2010. Antioxidant and antifungal properties of benzimidazole derivatives. Z. Naturforsch. 65, 537–542.

Kutzke, H., Al-Mansour, M., Klapper, H., 1996. Stable and metastable crystal phases of 4-methylbenzophenone. J. Mol. Struct. 374, 129–135.

Lee, C., Yang, W., Parr, G.R., 1988. Development of the Colle-Salvetti correlation-energy formula into a functional of the electron density. Phys. Rev. B 37, 785–789.

León-Carmona, J.R., Galano, A., 2011. Is caffeine a good scavenger of oxygenated free radicals? J. Phys. Chem. B 115, 4538–4546.

Mairesse, G., Boivin, J.C., Thomas, D.J., Bermann, M.C., Bonte, J.P., Lesieur, D., 1984. Structure de la benzoyl-6 dihydro-2,3 benzoxazole-1,3 one-2, $C_{14}H_9NO_3$. Acta Crystallogr. Sect. C 40, 1019–1020.

Maritim, A.C., Sanders, R.A., Watkins III, J.B., 2003. Diabetes, oxidative stress, and antioxidants: a review. J. Biochem. Mol. Toxicol. 17, 24–38.

Marnett, L.J., 1987. Peroxyl free radicals: potential mediator of tumor initiation and promotion. Carcinogenesis, Carcinogen. 8, 1365–1373.

Mavrova, A., Anichina, K., Vuchev, D., Tsenov, J., Kondeva, M., Mitcheva, M., 2005a. Synthesis and antitrichinellosis activity of some 2-substituted-[1,3]thiazolo[3,2*a*]benzimidazol-3(2*H*)-ones. Bioorg. Med. Chem. 13, 5550–5559.

Mavrova, A., Anichina, K., Vutchev, D., Tsenov, Y., Kondeva, M., Micheva, M., 2005b. Synthesis and antitrichinellosis activity of some 2-substituted-[1,3]thiazolo[3,2-a]benzimidazol-3(2H)-ones. Bioorg. Med. Chem. 13, 5550–5559.

Mavrova, A., Yancheva, D., Anastassova, N., Anichina, K., Zvezdanovic, J., Djordjevic, A., Markovic, D., Smelcerovic, A., 2015. Synthesis, electronic properties, antioxidant and antibacterial activity of some new benzimidazoles. Bioorg. Med. Chem. 23. 6317-6126.

Menteşea, E., Yılmaza, F., Baltaşa, N., Bekircanb, O., Kahvecic, B., 2015. Synthesis and antioxidant activities of some new triheterocyclic compounds containing benzimidazole, thiophene, and 1,2,4-triazole rings. J. Enzyme Inhib. Med. Chem. 30, 435–441.

Mitcheva, M., Kondeva, M., Vitcheva, V., Nedialkov, P., Kitanov, G., 2006. Effect of benzophenones from *Hypericum annulatum* on carbon tetrachloride-induced toxicity in freshly isolated rat hepatocytes. Redox Rep. 11, 3–8.

Mohamed, O., M'rabet, H., Hemissi, H., El Efrit, M., 2009. 2,2′-Bis (methylene)-3,3′-(2-thioxo-2,3-dihydro-1H-benzimidazole-1,3-diyl) dipropanenitrile. Acta Crystallogr. Sect. E: Crystallogr. Commun. 65, 2947.

Molinspiration Cheminformatics, 2015. www.molinspiration.com, Molinspiration property engine v2015.01.

Monika, G., Singh, S., Mohan, C., 2014. Benzimidazole: an emerging scaffold for analgesic and anti-inflammatory agents. Eur. J. Med. Chem. 76, 494–505.

Montserrat, M., Morales, A., Colell, A., García-Ruiz, C., Fernández-Checa, J., 2009. Mitochondrial glutathione, a key survival antioxidant. Antioxid. Redox Signal. 11, 2685–2700.

O'Donell, V., Burkit, M., 1994. Mitochondrial metabolism of a hydroperoxide to free radicals in human endothelial cells: an electron spin resonance spin-trapping investigation. Biochem. J. 304, 707–713.

Ollinger, K., Brunk, U., 1995. Cellular injury-induced by oxidative stress is mediated through lysosomal damage. Free Radical Biol. Med. 19, 565–574.

Patt, H., Tyree, E., Straube, L., Smith, D., 1949. Cysteine protection against X irradiation. Science 110, 213–214.

Paul, B., Snyder, S., 2010. The unusual amino acid L-ergothioneine is a physiologic cytoprotectant. Cell Death Differ. 17, 1134–1140.

Phiphatwatcharaded, C., Topark-Ngarm, A., Puthongking, P., Mahakunakorn, P., 2014. Anti-inflammatory activities of melatonin derivatives in lipopolysaccharide-stimulated RAW 264.7 cells and antinociceptive effects in mice. Drug Dev. Res. 75, 235–245.

Poli, G., Albano, E., Dianzani, M., 1987. The role of lipid peroxidation in liver damage. Chem. Phys. Lipids 45, 117–142.

Reed, A.E., Curtiss, L.A., Weinhold, F., 1988. Chem. Rev. 88, 899–926.

Refaat, H., 2010. Synthesis and anticancer activity of some novel 2-substituted benzimidazole derivatives. Eur. J. Med. Chem. 45, 2949–2956.

Rimarčík, J., Lukeš, V., Klein, E., Ilčin, M., 2010. Study of the solvent effect on the enthalpies of homolytic and heterolytic N—H bond cleavage in p-phenylenediamine and tetracyano-p-phenylenediamine. J. Mol. Struct. (Theochem) 952, 25–30.

Samuni, A., Aronovitch, J., Chevion, M., 1983. Metal-mediated hydroxyl radical damage. A site-specific mechanism, in oxidative damage and related enzymes. Life Chem. Rep. 2, 39–47.

Saxena, D., Khajuria, R., Suri, O., 1982. Synthesis and spectral studies of 2-mercaptobenzimidazole derivatives. J. Heterocycl. Chem. 18, 681–683.

Sheldrick, G.M., 2008. A short history of SHELX. Acta Cryst. A 64, 112–122.

Shin, J.M., Kim, N., 2013. Pharmacokinetics and pharmacodynamics of the proton pump inhibitors. Neurogastroenterol. Motil. 19, 25–35.

Shirinzadeh, H., Eren, B., Gurer-Orhan, H., Suzen, S., Özden, S., 2010. Novel indole-based analogs of melatonin: synthesis and in vitro antioxidant activity studies. Molecules 15, 2187–2202.

Singh, N., Pandurangan, A., Rana, K., Anand, P., Ahamad, A., Tiwari, A.K., 2012. Benzimidazole: a short review of their antimicrobial activities. Int. Curr. Pharm. J. 1, 119–127.

Smith, D.M., 2008. Dihydrobenzimidazoles, benzimidazolones, benzimidazolethiones and related compounds. In: Preston, P.N. (Ed.), Chemistry of Heterocyclic Compounds: Benzimidazoles and Cogeneric Tricyclic Compounds, Part 1, vol. 40. John Wiley & Sons, New York, pp. 331–389.

Solar, S., Getoff, N., Surdhar, P.S., Armstrong, D.A., Singh, A., 1991. Oxidation of tryptophan a nd N-methylindole by N3, Br 2, (SNC)2 radicals in light and heavy water solutions. A pulse radiolysis study. J. Phys. Chem. 95, 3639–3643.

Stephens, J.W., Priorm, S.L., 2015. Cardiovascular and metabolic disease: scientific discoveries and new therapies. R. Soc. Chem. Cambridge. Struct Chem. 26, 831–844.

Taha, M., Ismail, N.H., Imran, S., Mohamad, M.H., Wadood, A., Rahim, F., Saad, S.M., Rehman, A., Khan, K.M., 2016. Synthesis, α-glucosidase inhibitory, cytotoxicity and docking studies of 2-aryl-7-methylbenzimidazoles. Bioorg. Chem. 65, 100–109.

Takayama, F., Egashira, T., Yamanaka, Y., 2001. Protective effect of Ninjin-yoei-to on damage to isolated hepatocytes following transient exposure to *tert*-butyl hydroperoxide. Jpn. J. Pharmacol. 85, 227–233.

Tonelli, M., Paglietti, G., Boido, V., Sparatore, F., Marongiu, F., Marongiu, E., Colla, La., Loddo, R., 2008. Antviral activity of benzimidazole derivatives. I. Antiviral activity of 1-substituted-2-[(benzotriazol-1/2-yl)methyl]benzimidazoles. Chem. Biodiversity 5, 2386–2401.

Tonelli, M., Simone, M., Tasso, B., Novelli, F., Boido, V., Sparatore, F., Paglietti, G., Pricl, S., Giliberti, G., Blois, S., Ibba, C., Sanna, G., Loddo, R., La Colla, P., 2010. Antiviral activity of benzimidazole derivatives. II. Antiviral activity of 2-phenylbenzimidazole derivatives. Bioorg. Med. Chem. 18, 2937–2953.

Vagánek, A., Rimarcík, J., Lukeš, V., Klein, E., 2012. On the energetics of homolytic and heterolytic O—H bond cleavage in flavonoids. Comput. Theor. Chem. 991, 192–200.

Valko, M., Rhodes, C., Moncol, J., Izakovic, M., Mazur, M., 2006. Free radicals, metals and antioxidants in oxidative stress-induced cancer. Chem.-Biol. Interact. 160, 1–40.

Velkov, Y.Z., Galunska, B.T., Paskalev, D.N., Tadjer, A.V., 2009. Melatonin: quantum-chemical and biochemical investigation of antioxidant activity. Eur. J. Med. Chem. 44, 2834–2839.

Vyas, V., Ghate, M., 2010. Substituted benzimidazole derivatives as angiotensin II-AT1 receptor antagonist: a review. Mini. Rev. Med. Chem. 10, 1366–1384.

Weinhold, F., Carpenter, J.E., 1988. The natural bond orbital lewis structure concept for molecules, radicals, and radical ions. In: Naaman, R., Vager, Z. (Eds.), The Structure of Small Molecules and Ion. Plenum, New York, pp. 227–236.

Zawawi, N.K.N.A., Taha, M., Ahmat, N., Wadood, A., Ismail, N.H., Rahim, F., Azam, S.S., Abdullah, N., 2016. Benzimidazole derivatives as new α-glucosidase inhibitors and in silico studies. Bioorg. Chem. 64, 29–36.

Zawawi, N.K.N.A., Taha, M., Ahmat, N., Wadood, A., Ismail, N.H., Rahim, F., Ali, M., Abdullah, N., Khan, K.M., 2015. Novel 2,5-disubtituted-1,3,4-oxadiazoles with benzimidazole backbone: a new class of β-glucuronidase inhibitors and in silico studies. Bioorg. Med. Chem. 23, 3119–3125.